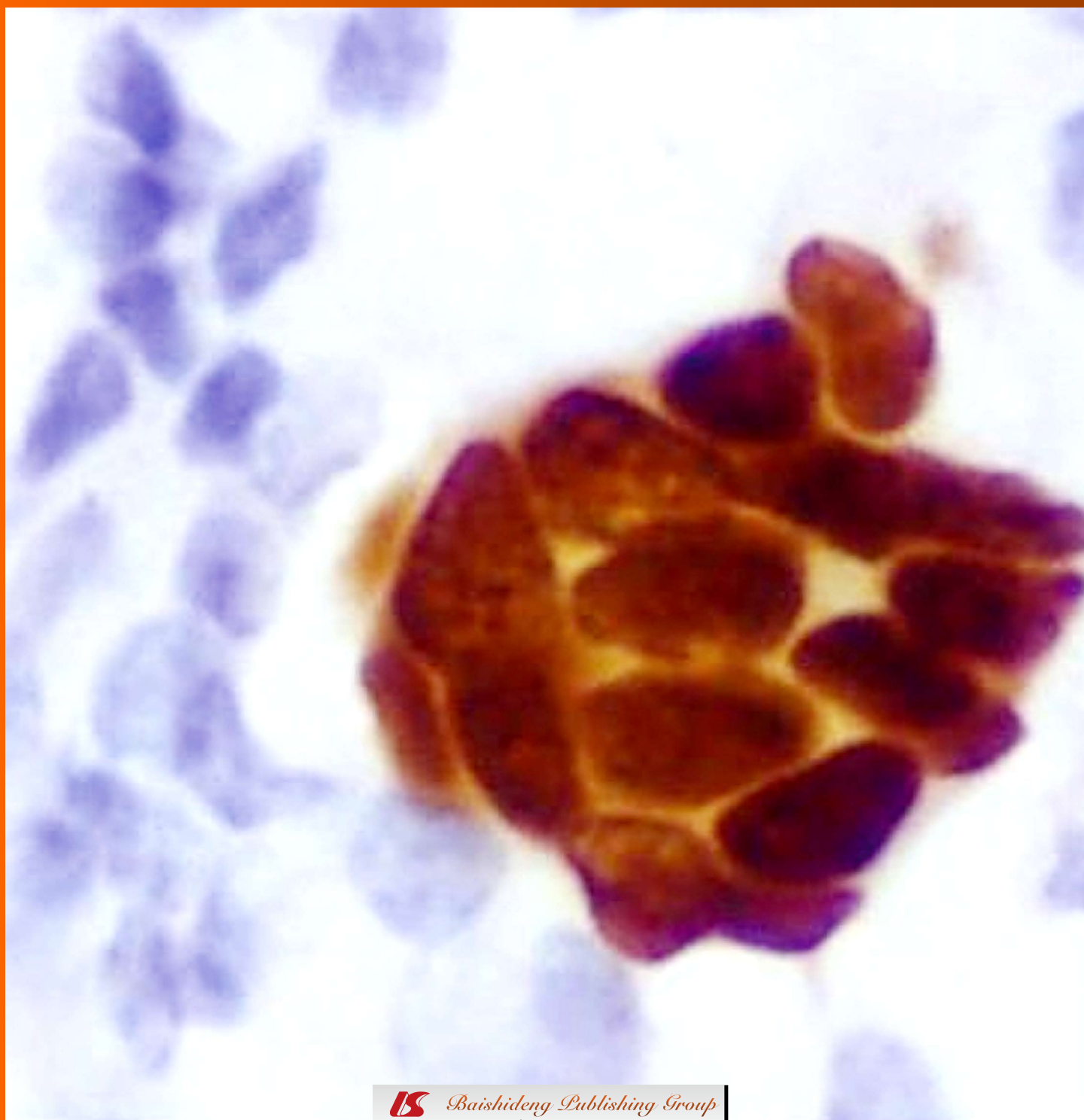


World Journal of *Clinical Oncology*

World J Clin Oncol 2011 April 10; 2(4): 169-194



Editorial Board

2010-2014

The *World Journal of Clinical Oncology* Editorial Board consists of 316 members, representing a team of worldwide experts in oncology. They are from 33 countries, including Australia (6), Belgium (2), Brazil (1), Canada (5), China (34), Egypt (2), Finland (1), France (4), Germany (14), Greece (7), Hungary (1), India (5), Iran (1), Israel (2), Italy (27), Japan (20), Malaysia (1), Mexico (1), Netherlands (6), New Zealand (1), Peru (1), Poland (1), Portugal (4), Saudi Arabia (1), Singapore (9), South Korea (7), Spain (7), Sweden (1), Switzerland (2), Thailand (2), Turkey (6), United Kingdom (11), and United States (123).

PRESIDENT AND EDITOR-IN-CHIEF

Lian-Sheng Ma, *Beijing*

STRATEGY ASSOCIATE EDITORS-IN-CHIEF

Robert J Amato, *Houston*

Kapil Mehta, *Houston*

E YK Ng, *Singapore*

Masahiko Nishiyama, *Saitama*

María Paez de la Cadena, *Vigo*

GJ Peters, *Amsterdam*

Bruno Sangro, *Pamplona*

Wolfgang A Schulz, *Düsseldorf*

Vaclav Vetvicka, *Louisville*

Giuseppe Visani, *Pesaro*

GUEST EDITORIAL BOARD MEMBERS

Shih-Chieh Chang, *Taichung*

How-Ran Guo, *Tainan*

Chao-Cheng Huang, *Kaohsiung*

Chia-Hung Kao, *Taichung*

Shiu-Ru Lin, *Kaohsiung*

Chih-Hsin Tang, *Taichung*

Chih-En Tseng, *Chiayi*

Jaw-Yuan Wang, *Kaohsiung*

Tzu-Chen Yen, *Taoyuan*

Mei-Chin Yin, *Taichung*

Shyng-Shiou F Yuan, *Kaohsiung*

MEMBERS OF THE EDITORIAL BOARD



Australia

Suzanne K Chambers, *Brisbane*

Thomas Grewal, *Sydney*

Peter Hersey, *Newcastle*

Liang Qiao, *Sydney*

Des R Richardson, *Sydney*



Belgium

Tim Van den Wyngaert, *Edegem*

Jan B Vermorken, *Edegem*



Brazil

Gustavo Arruda Viani, *Marilia*



Canada

Dimcho Bachvarov, *Quebec*

Slimane Belbraouet, *Moncton*

Vera Hirsh, *Montreal*

Jennifer Spratlin, *Edmonton*

Seang Lin Tan, *Montreal*



China

Xiao-Tian Chang, *Jinan*

George G Chen, *Hong Kong*

Lei Chen, *Beijing*

Xiao-Ping Chen, *Wuhan*

Yick-Pang Ching, *Hong Kong*

William CS Cho, *Hong Kong*

Yong-Song Guan, *Chengdu*

Lun-Xiu Qin, *Shanghai*

John A Rudd, *Hong Kong*

Jian-Yong Shao, *Guangzhou*

Eric Tse, *Hong Kong*

Gary M Tse, *Hong Kong*

Cheuk Wah, *Hong Kong*

Ming-Rong Wang, *Beijing*

Wei-Hong Wang, *Beijing*

Xun-Di Xu, *Changsha*

Thomas Yau, *Hong Kong*

Qi-Nong Ye, *Beijing*

Anthony PC Yim, *Hong Kong*

Man-Fung Yuen, *Hong Kong*

Ke Zen, *Nanjing*

Xue-Wu Zhang, *Guangzhou*



Egypt

Mohamed Nasser Elsheikh, *Tanta*

Ashraf A Khalil, *Alexandria*



Finland

Veli-Matti Kähäri, *Turku*



France

René Adam, *Villejuif*

Claude Caron de Fromental, *Lyon*

Nathalie Lassau, *Villejuif*

Michel Meignan, *Créteil*



Germany

Thomas Bock, *Berlin*

Christiane Josephine Bruns, *Munich*

Markus W Büchler, *Heidelberg*

André Eckardt, *Hannover*

Felix JF Herth, *Heidelberg*

Georg Kähler, *Mannheim*

Robert Mandic, *Marburg*
Klaus Mross, *Freiburg*
Lars Mueller, *Kiel*
Katharina Pachmann, *Jena*
Matthias Peiper, *Düsseldorf*
Gerd J Ridder, *Freiburg*
Harun M Said, *Wuerzburg*



Greece

Leonidas Duntas, *Athens*
Nicholas Pavlidis, *Ioannina*
Professor A Polyzos, *Athens*
Alexander D Ravidis, *Athens*
Evangelia Razis, *Athens*
Dimitrios Roukos, *Ioannina*
Kostas Syrigos, *Athens*



Hungary

Zsuzsa Schaff, *Budapest*



India

Tanya Das, *Kolkata*
G Arun Maiya, *Manipal*
Ravi Mehrotra, *Allahabad*
Sanjeeb K Sahoo, *Bhubaneswar*
Sarwat Sultana, *New Delhi*



Iran

Ali Kabir, *Tehran*



Israel

Avi Hefetz Khafif, *Tel-Aviv*
Doron Kopelman, *Caesarea*



Italy

Luca Arcaini, *Pavia*
Enrico Benzoni, *Tolmezzo*
Rossana Berardi, *Ancona*
Valentina Bollati, *Milan*
Emilio Bria, *Rome*
Guido Cavaletti, *Monza*
Paolo Chieffi, *Naples*
Marco Ciotti, *Rome*
Giuseppe G Di Lorenzo, *Naples*
Alfio Ferlito, *Udine*
Daris Ferrari, *Abbiategrasso*
Alessandro Franchi, *Florence*
Gennaro Galizia, *Naples*
Roberto Mazzanti, *Firenze*
Michele N Minuto, *Pisa*
Simone Mocellin, *Padova*
Nicola Normanno, *Naples*
Marco G Paggi, *Rome*
Domenico Rubello, *Rovigo*
Antonio Russo, *Palermo*
Daniele Santini, *Rome*
Bruna Scaggiante, *Trieste*

Riccardo Schiavina, *Bologna*
Enzo Spisni, *Bologna*
Bruno Vincenzi, *Rome*
Giovanni Vitale, *Cusano Milanino*



Japan

Hidefumi Aoyama, *Niigata*
Takaaki Arigami, *Kagoshima*
Narikazu Boku, *Shizuoka*
Kazuaki Chikamatsu, *Chuo*
Toru Hiyama, *Higashihiroshima*
Satoru Kakizaki, *Gunma*
Shuichi Kaneko, *Kanazawa*
Koji Kawakami, *Kyoto*
Hiroki Kuniyasu, *Kashihara*
Eiji Miyoshi, *Suita*
Toru Mukohara, *Kobe*
Atsushi Nakajima, *Tokyo*
Takahide Nakazawa, *Sagamihara*
Seishi Ogawa, *Tokyo*
Youngjin Park, *Chiba prefecture*
Naoya Sakamoto, *Tokyo*
Hidekazu Suzuki, *Tokyo*
Michiko Yamagata, *Shimotsuga-gun*
Hiroki Yamaue, *Wakayama*



Malaysia

Min-Tze Liong, *Penang*



Mexico

Rafael Moreno-Sanchez, *Mexico*



Netherlands

Jurgen J Futterer, *Nijmegen*
Bart M Gadella, *Utrecht*
Johannes A Langendijk, *Groningen*
IM Verdonck-de Leeuw, *Amsterdam*
J Voortman, *Amsterdam*



New Zealand

Joanna Skommer, *Auckland*



Peru

Henry L Gomez, *Lima*



Poland

Lukasz Wicherek, *Bydgoszcz*



Portugal

Antonio Araujo, *Porto*
Rui M Medeiros, *Porto*
Paula Ravasco, *Lisbon*
Rui Manuel Reis, *Braga*



Saudi Arabia

Shahab Uddin, *Riyadh*



Singapore

Wei Ning Chen, *Singapore*
John M Luk, *Singapore*
Shu Wang, *Singapore*
Celestial Yap, *Singapore*
Khay-Guan Yeoh, *Singapore*
George W Yip, *Singapore*
Yong Zhang, *Singapore*
Zhan Zhang, *Singapore*



South Korea

Ho-Seong Han, *Seoul*
Young-Seoub Hong, *Busan*
Ja Hyeon Ku, *Seoul*
Geon Kook Lee, *Goyang-si*
Jae Cheol Lee, *Seoul*
Woo Sung Moon, *Jeonju*
Hyun Ok Yang, *Gangeung*



Spain

Maurizio Bendandi, *Pamplona*
Joan Carles, *Barcelona*
Javier Cortés Castán, *Barcelona*
Jose M Cuezva, *Madrid*
Jesús Prieto, *Pamplona*



Sweden

Lalle Hammarstedt, *Stockholm*



Switzerland

A Lugli, *Basel*
Jacqueline Schoumans, *Lausanne*



Thailand

Sueb Wong Chuthapisith, *Bangkok*
Songsak Petmitr, *Bangkok*



Turkey

Nejat Dalay, *Istanbul*
Seher Demirer, *Ankara*
Zafer Özgür Pektaş, *Adana*
Alper Sevinc, *Gaziantep*
Engin Ulukaya, *Gorukle Bursa*
Isik G Yulug, *Ankara*



United Kingdom

Shahriar Behboudi, *London*
Alastair David Burt, *Newcastle*

Barbara Guinn, *Southampton*
Stephen Hiscox, *Cardiff*
Wen G Jiang, *Cardiff*
Youqiang Ke, *Liverpool*
Charles H Lawrie, *Oxford*
T H Marczylo, *Leicester*
Simon N Rogers, *Liverpool*
Abeezar I Sarela, *Leeds*
Alex Tonks, *Cardiff*



United States

Ali Syed Arbab, *Detroit*
Athanassios Argiris, *Pittsburgh*
Raffaele Baffa, *Gaithersburg*
Partha P Banerjee, *Washington*
Scott M Belcher, *Cincinnati*
Heather A Bruns, *Muncie*
Deliang Cao, *Springfield*
William E Carson III, *Columbus*
Disaya Chavalitdhamrong, *Bronx*
Jason Chen, *New York*
Oliver Chen, *Boston*
Jin Q Cheng, *Tampa*
Bruce D Cheson, *Washington*
Mei-Sze Chua, *Stanford*
Muzaffer Cicek, *Rochester*
Ezra EW Cohen, *Chicago*
Hengmi Cui, *Baltimore*
Q Ping Dou, *Detroit*
David W Eisele, *San Francisco*
Wafik S El-Deiry, *Hershey*
Mahmoud El-Tamer, *New York*
Armin Ernst, *Boston*
Zeev Estrov, *Houston*
Marwan Fakih, *Buffalo*
Michelle A Fanale, *Houston*
Xianjun Fang, *Richmond*
Benjamin L Franc, *Sacramento*
Giulia Fulci, *Boston*
David H Garfield, *Denver*
Antonio Giordano, *Philadelphia*
S Murty Goddu, *St. Louis*
Yun Gong, *Houston*
Lei Guo, *Jefferson*
Sanjay Gupta, *Cleveland*
Subrata Haldar, *Cleveland*
Sam M Hanash, *Seattle*
Randall E Harris, *Columbus*
Andrea A Hayes-Jordan, *Houston*
David W Hein, *Louisville*
Paul J Higgins, *Albany*
James R Howe, *Iowa*
Hedvig Hricak, *New York*
Chuanshu Huang, *Tuxedo*
Wendong Huang, *Duarte*
Naijie Jing, *Houston*
Masao Kaneki, *Charlestown*
Hagop Kantarjian, *Houston*
Maria C Katapodi, *Ann Arbor*
Mark R Kelley, *Indianapolis*
Venkateshwar G Keshamouni, *Ann Arbor*
Nikhil Ishwar Khushalani, *Buffalo*
Arianna L Kim, *New York*
K Sean Kimbro, *Atlanta*
Leonidas G Koniaris, *Miami*
Hasan Korkaya, *Ann Arbor*
Sunil Krishnan, *Houston*
Melanie H Kucherlapati, *Boston*
Paul C Kuo, *Maywood*
Andrew C Larson, *Chicago*
Felix Leung, *North Hills*
Ho-Sheng Lin, *Detroit*
Jennifer Lin, *Boston*
Shiaw-Yih Lin, *Houston*
Steven E Lipshultz, *Miami*
Bolin Liu, *Aurora*
Jeri A Logemann, *Evanston*
Bert Lum, *South San Francisco*
Jian-Hua Luo, *Pittsburgh*
Shyamala Maheswaran, *Charlestown*
David L McCormick, *Chicago*
Murielle Mimeault, *Omaha*
Monica Mita, *San Antonio*
Gerard E Mullin, *Baltimore*
Ravi Murthy, *Houston*
Jacques E Nör, *Ann Arbor*
James S Norris, *Charleston*
Scott Okuno, *Rochester*
Timothy Michael Pawlik, *Baltimore*
Joseph A Paydarfar, *Lebanon*
Jay J Pillai, *Baltimore*
Luis F Porrata, *Rochester*
Raj S Pruthi, *Chapel Hill*
Jianyu Rao, *Los Angeles*
Steven A Rosenzweig, *Charleston*
Eric Rowinsky, *Warren*
Jose Russo, *Philadelphia*
Stephen H Safe, *College Station*
Adnan Said, *Madison*
Stewart Sell, *Albany*
Shahrokh F Shariat, *New York*
Jing Shen, *New York*
Dong Moon Shin, *Atlanta*
Haval Shirwan, *Louisville*
Viji Shridhar, *Rochester*
Anurag Singh, *Buffalo*
Lawrence J Solin, *Philadelphia*
David R Spigel, *Nashville*
Brendan Curran Stack, *Little Rock*
Charles F Streckfus, *Houston*
Lu-Zhe Sun, *San Antonio*
Vladimir N Uversky, *Indianapolis*
Jean-Nicolas Vauthey, *Houston*
Hanlin L Wang, *Los Angeles*
Thomas D Wang, *Ann Arbor*
Dennis D Weisenburger, *Omaha*
Robert P Whitehead, *Las Vegas*
Juergen K Willmann, *Stanford*
Jason D Wright, *New York*
Q Jackie Wu, *Durham*
Shenhong Wu, *Stony Brook*
Hang Xiao, *Amherst*
Mingzhao Xing, *Baltimore*
Ronald Xiaorong Xu, *Columbus*
Kaiming Ye, *Fayetteville*
William Andrew Yeudall, *Richmond*
Dihua Yu, *Houston*
Bao-Zhu Yuan, *Morgantown*
Yawei Zhang, *New Haven*
Weixiong Zhong, *Madison*
Shufeng Zhou, *Tampa*
Yue Zou, *Johnson*

Contents

Monthly Volume 2 Number 4 April 10, 2011

EDITORIAL

- 169 Imaging as a diagnostic and therapeutic tool in clinical oncology
Ng EYK, Acharya RU

TOPIC HIGHLIGHT

- 171 Breast imaging: A survey
Vinitha Sree S, Ng EYK, Acharya RU, Faust O
- 179 Online volume rendering of incrementally accumulated LSCEM images for superficial oral cancer detection
Chiew WM, Lin F, Qian K, Seah HS

ORIGINAL ARTICLES

- 187 Automation of immunohistochemical evaluation in breast cancer using image analysis
Prasad K, Tiwari A, Ilanthodi S, Prabhu G, Pai M

ACKNOWLEDGMENTS I Acknowledgments to reviewers of *World Journal of Clinical Oncology*

APPENDIX I Meetings
 I-V Instructions to authors

ABOUT COVER Prasad K, Tiwari A, Ilanthodi S, Prabhu G, Pai M. Automation of immunohistochemical evaluation in breast cancer using image analysis.
World J Clin Oncol 2011; 2(4): 187-194
<http://www.wjgnet.com/2218-4333/full/v2/i4/187.htm>

AIM AND SCOPE *World Journal of Clinical Oncology* (*World J Clin Oncol*, *WJCO*, online ISSN 2218-4333, DOI: 10.5306) is a monthly peer-reviewed, online, open-access, journal supported by an editorial board consisting of 316 experts in oncology from 33 countries.
 The aim of *WJCO* is to report rapidly new theories, methods and techniques for prevention, diagnosis, treatment, rehabilitation and nursing in the field of oncology. *WJCO* covers etiology, epidemiology, evidence-based medicine, informatics, diagnostic imaging, endoscopy, tumor recurrence and metastasis, tumor stem cells, radiotherapy, chemotherapy, interventional radiology, palliative therapy, clinical chemotherapy, biological therapy, minimally invasive therapy, physiotherapy, psycho-oncology, comprehensive therapy, oncology-related traditional medicine, integrated Chinese and Western medicine, and nursing. *WJCO* covers tumors in various organs/tissues, including the female reproductive system, bone and soft tissue, respiratory system, urinary system, endocrine system, skin, breast, nervous system, head and neck, digestive system, and hematologic and lymphatic system.

FLYLEAF I-III Editorial Board

EDITORS FOR THIS ISSUE

Responsible Assistant Editor: *Na Liu*
 Responsible Electronic Editor: *Wen-Hua Ma*
 Proofing Editor-in-Chief: *Lian-Sheng Ma*
 Responsible Science Editor: *Lin Tian*

NAME OF JOURNAL
World Journal of Clinical Oncology

LAUNCH DATE
 November 10, 2010

SPONSOR
 Beijing Baishideng BioMed Scientific Co., Ltd.,
 Room 903, Building D, Ocean International Center,
 No. 62 Dongsihuan Zhonglu, Chaoyang District,
 Beijing 100025, China
 Telephone: +86-10-8538-1892
 Fax: +86-10-8538-1893
 E-mail: baishideng@wjgnet.com
<http://www.wjgnet.com>

EDITING
 Editorial Board of *World Journal of Clinical Oncology*,
 Room 903, Building D, Ocean International Center,
 No. 62 Dongsihuan Zhonglu, Chaoyang District,
 Beijing 100025, China
 Telephone: +86-10-5908-0036
 Fax: +86-10-8538-1893
 E-mail: wjco@wjgnet.com
<http://www.wjgnet.com>

PUBLISHING
 Baishideng Publishing Group Co., Limited,
 Room 1701, 17/F, Henan Building,
 No.90 Jaffe Road, Wanchai, Hong Kong, China
 Fax: +852-3115-8812
 Telephone: +852-5804-2046

E-mail: baishideng@wjgnet.com
<http://www.wjgnet.com>

SUBSCRIPTION
 Beijing Baishideng BioMed Scientific Co., Ltd.,
 Room 903, Building D, Ocean International Center,
 No. 62 Dongsihuan Zhonglu, Chaoyang District,
 Beijing 100025, China
 Telephone: +86-10-8538-1892
 Fax: +86-10-8538-1893
 E-mail: baishideng@wjgnet.com
<http://www.wjgnet.com>

PUBLICATION DATE
 April 10, 2011

ISSN
 ISSN 2218-4333 (online)

PRESIDENT AND EDITOR-IN-CHIEF
 Lian-Sheng Ma, *Beijing*

STRATEGY ASSOCIATE EDITORS-IN-CHIEF
 Robert J Amato, *Houston*
 Maria Paez de la Cadena, *Vigo*
 Kapil Mehta, *Houston*
 E YK Ng, *Singapore*
 Masahiko Nishiyama, *Saitama*
 GJ Peters, *Amsterdam*
 Bruno Sangro, *Pamplona*
 Wolfgang A Schulz, *Düsseldorf*
 Vaclav Vetvicka, *Louisville*
 Giuseppe Visani, *Pesaro*

EDITORIAL OFFICE

Lin Tian, Director
World Journal of Clinical Oncology
 Room 903, Building D, Ocean International Center,
 No. 62 Dongsihuan Zhonglu, Chaoyang District,
 Beijing 100025, China
 Telephone: +86-10-8538-1892
 Fax: +86-10-8538-1893
 E-mail: wjco@wjgnet.com
<http://www.wjgnet.com>

COPYRIGHT

© 2011 Baishideng. Articles published by this Open-Access journal are distributed under the terms of the Creative Commons Attribution Non-commercial License, which permits use, distribution, and reproduction in any medium, provided the original work is properly cited, the use is non commercial and is otherwise in compliance with the license.

SPECIAL STATEMENT

All articles published in this journal represent the viewpoints of the authors except where indicated otherwise.

INSTRUCTIONS TO AUTHORS

Full instructions are available online at http://www.wjgnet.com/2218-4333/g_info_20100722172206.htm

ONLINE SUBMISSION

<http://www.wjgnet.com/2218-4333office>

Imaging as a diagnostic and therapeutic tool in clinical oncology

Eddie Yin-Kwee Ng, Rajendra U Acharya

Eddie Yin-Kwee Ng, School of Mechanical and Aerospace Engineering, College of Engineering, Nanyang Technological University, 50, Nanyang Avenue, Singapore 639798, Singapore
Rajendra U Acharya, School of Engineering, Ngee Ann Polytechnic, Singapore 599489, Singapore

Author contributions: Ng EYK and Acharya RU contributed equally to this editorial.

Correspondence to: Eddie Yin-Kwee Ng, PhD, PGDTHE, Associate Professor, School of Mechanical and Aerospace Engineering, College of Engineering, Nanyang Technological University, 50, Nanyang Avenue, Singapore 639798, Singapore. mykng@ntu.edu.sg

Telephone: +65-65-67904455 Fax: +65-65-67911859

Received: March 18, 2010 Revised: March 31, 2011

Accepted: April 7, 2011

Published online: April 10, 2011

Abstract

According to the WHO report published in 2010, about 13% of all deaths are due to cancer. Of these, lung, liver, stomach, colon and breast cancer are the most prevalent. It was also reported that about 30% of the deaths due to cancer can be avoided, if diagnosed and treated early. Hence, there is an urgent need to diagnose these cancers efficiently. Various imaging and therapeutic methods have been proposed and used to accurately detect cancer. In this special two issues, there are eight papers covering different aspects of oncology using various imaging or therapeutic methods.

© 2011 Baishideng. All rights reserved.

Key words: Imaging; Clinical oncology

Ng EYK, Acharya RU. Imaging as a diagnostic and therapeutic tool in clinical oncology. *World J Clin Oncol* 2011; 2(4): 169-170
Available from: URL: <http://www.wjgnet.com/2218-4333/full/v2/i4/169.htm> DOI: <http://dx.doi.org/10.5306/wjco.v2.i4.169>

techniques over the last 50 years. Various endoscopic models have been designed and developed which differ in their ability to inspect the inner surfaces of the body cavities. Furthermore, the rigid nature of such endoscopes and the need for high resolution imaging has enabled researchers to develop more sophisticated flexible probes for medical and single cell imaging for early disease diagnosis. In this special two issues, there are eight papers covering different aspects of oncology using various imaging or therapeutic methods.

Paper 1^[1] introduces the background of optical spectroscopy in cancer management, which includes the advantages of this technique compared with other established techniques, the principle of optical spectroscopy and the typical instrumentation setup. Current progress in optical spectroscopy for the diagnosis of cancer in the brain, breast, cervix, lung, stomach, colon, prostate and skin are reviewed. A few commercially available clinical instruments based on optical spectroscopy techniques are presented. Several technical challenges and standard issues are also discussed.

A preliminary system to perform online rendering side-by-side with laser scanning confocal endomicroscopic imaging is presented in Paper 2^[2]. By having an immediate knowledge of the dataset quality as well as the biological tissue conditions, alterations can be made on the spot. This will introduce the opportunity to change imaging conditions or medical decisions according to the online rendering results. This work is also motivated by the need to realize the quality of the captured datasets in real time to reduce excessive time required for offline rendering.

Imaging of gastroenteropancreatic neuroendocrine tumors can be broadly divided into anatomic and functional techniques. Anatomic imaging determines the local extent of the primary lesion, providing crucial information required for surgical planning. Functional imaging not only determines the extent of metastatic disease spread, but also provides important information with regards to the biologic behavior of the tumor, allowing clinicians to decide on the most appropriate forms of treatment. Paper

Medical imaging and diagnostics have been established

3^[3] reviews the current literature on this subject, with an emphasis on the strengths of each imaging modality.

Existing imaging modalities for breast cancer screening, diagnosis and therapy monitoring, namely X-ray mammography and magnetic resonance imaging (MRI), have been proven to have limitations. Diffuse optical imaging, a set of non-invasive imaging modalities using near-infrared light, may be an alternative, if not a replacement, to those existing modalities. Paper 4^[4] covers the background knowledge, recent clinical trial outcome, and the future outlook of this newly emerging medical imaging modality.

Paper 5^[5] presents a technique for automation in the diagnosis of breast cancer from immunohistochemically stained biopsy specimens. It has been demonstrated through this work that manual evaluation introduces a number of variations, whereas automated analysis provides objective evaluation and is repeatable. Such automation can facilitate fast and efficient diagnosis of breast cancer cases and eliminate human errors to a large extent.

Efforts have been made to improve the accuracy of breast cancer diagnosis using different imaging modalities. Ultrasound and MRI have been used to detect breast cancers in high risk patients. Recently, electrical impedance imaging and nuclear medicine techniques are also being widely used for breast cancer screening and diagnosis. Paper 6^[6] discusses the capabilities of various breast imaging modalities.

Paper 7^[7] proposes techniques to investigate the strength of support vector regression in cancer prognosis using imaging features. In this work, the authors have used the combinational methods of Support Vector Classification-

Regression, feature selection, and sampling that can improve cancer prognosis. More significant features may further enhance cancer prognosis accuracy.

The clinical outcomes of high intensity focused ultrasound (HIFU) ablation applied to cancers are discussed. The current challenges in the application of HIFU in tumor treatment, such as HIFU-mediated drug delivery, vessel occlusion, and soft tissue erosion (“histotripsy”) are discussed in paper 8^[8].

We hope that the papers in this special issue will help to disseminate knowledge in the field of clinical oncology.

REFERENCES

- 1 **Liu Q.** Role of optical spectroscopy using endogenous contrasts in clinical cancer diagnosis. *World J Clin Oncol* 2011; **2**: 50-63
- 2 **Chiew WM,** Lin F, Qian K, Seah HS. Online volume rendering of incrementally accumulated LSCEM images for superficial oral cancer detection. *World J Clin Oncol* 2011; **2**: 179-186
- 3 **Tan EH,** Tan CH. Imaging of gastroenteropancreatic neuroendocrine tumors. *World J Clin Oncol* 2011; **2**: 28-43
- 4 **Lee K.** Optical mammography: Diffuse optical imaging of breast cancer. *World J Clin Oncol* 2011; **2**: 64-72
- 5 **Prasad K,** Tiwari A, Ilanthodi S, Prabhu G, Pai M. Automation of immunohistochemical evaluation in breast cancer using image analysis. *World J Clin Oncol* 2011; **2**: 187-194
- 6 **Vinitha Sree S,** Ng EYK, Acharya RU, Faust O. Breast imaging: A survey. *World J Clin Oncol* 2011; **2**: 171-178
- 7 **Du X,** Dua S. Cancer prognosis using support vector regression in imaging modality. *World J Clin Oncol* 2011; **2**: 44-49
- 8 **Zhou YF.** High intensity focused ultrasound in clinical tumor ablation. *World J Clin Oncol* 2011; **2**: 8-27

S- Editor Tian L L- Editor Webster JR E- Editor Ma WH

Eddie Yin-Kwee Ng, PhD, PGDTHE, Associate Professor, Series Editor

Breast imaging: A survey

Subbhuraam Vinitha Sree, Eddie Yin-Kwee Ng, Rajendra U Acharya, Oliver Faust

Subbhuraam Vinitha Sree, Eddie Yin-Kwee Ng, School of Mechanical and Aerospace Engineering, Nanyang Technological University, Singapore 639798, Singapore

Rajendra U Acharya, Oliver Faust, Department of Electronics and Computer Engineering, Ngee Ann Polytechnic, Singapore 599489, Singapore

Author contributions: All the authors have equally contributed to writing the text and formatting the paper.

Correspondence to: Eddie Yin-Kwee Ng, PhD, PGDTHE, Associate Professor, School of Mechanical and Aerospace Engineering, Nanyang Technological University, Singapore 639798, Singapore. mykng@ntu.edu.sg

Telephone: +65-6790-4455 Fax: +65-6791-1859

Received: October 15, 2010 Revised: January 7, 2011

Accepted: January 14, 2011

Published online: April 10, 2011

Arbab, MD, PhD, Associate Scientist and Director, Cellular and Molecular Imaging Laboratory, Department of Radiology, Henry Ford Hospital, 1 Ford Place, 2F, Box 82, Detroit, MI 48202, United States; Slimane Belbraouet, PhD, Professeur Titulaire, Directeur, École des sciences des aliments, de nutrition et d'études familiales, Université de Moncton, Moncton, NB, E1A 3E9, Canada

Vinitha Sree S, Ng EYK, Acharya RU, Faust O. Breast imaging: A survey. *World J Clin Oncol* 2011; 2(4): 171-178 Available from: URL: <http://www.wjgnet.com/2218-4333/full/v2/i4/171.htm> DOI: <http://dx.doi.org/10.5306/wjco.v2.i4.171>

Abstract

Breast cancer is the second leading cause of death in women. It occurs when cells in the breast start to grow out of proportion and invade neighboring tissues or spread throughout the body. Mammography is one of the most effective and popular modalities presently used for breast cancer screening and detection. Efforts have been made to improve the accuracy of breast cancer diagnosis using different imaging modalities. Ultrasound and magnetic resonance imaging have been used to detect breast cancers in high risk patients. Recently, electrical impedance imaging and nuclear medicine techniques are also being widely used for breast cancer screening and diagnosis. In this paper, we discuss the capabilities of various breast imaging modalities.

© 2011 Baishideng. All rights reserved.

Key words: Breast cancer; Breast magnetic resonance imaging; Breast ultrasound; Mammography; Thermography**Peer reviewer:** Gary M Tse, MD, Department of Anatomical and Cellular Pathology, Prince of Wales Hospital, The Chinese University of Hong Kong, Shatin, Hong Kong, China; Ali Syed

INTRODUCTION

Breast cancer starts in the breast cells of both women and men. Worldwide, breast cancer is the second most common type of cancer after lung cancer (10.9% of cancer incidence in both men and women)^[1] and the fifth most common cause of cancer death^[2]. The National Breast Cancer Foundation has estimated around 200 000 new breast cancer cases and 40 000 deaths every year in women. In men, these statistics are 1700 and 450, respectively^[3]. According to the National Cancer Institute, an estimated 207 090 new cases and 39 840 deaths from breast cancer (only women) are expected to occur in the United States, despite recent advances in treatment^[4]. Given such circumstances, early diagnosis of breast cancer is considered vital, because statistics have shown a five-year survival rate of 96% for those whose cancer was detected in the early stages^[3].

The breast is composed of identical tissues in both men and women, and hence, breast cancer also occurs in men. Breast cancer incidence in men is approximately 100 times less than in women, but men with breast cancer are considered to have the same statistical survival rates as women^[5-7].

In this paper, our focus is on breast cancer detection modalities which use breast images obtained by various techniques for analysis and subsequent detection. For

better survival odds and reduced use of treatments and therapies and, therefore, fewer side-effects, many imaging modalities are continually being developed to diagnose this disease as early as possible. Some of these modalities are used for screening purposes, some for diagnostic purposes, and a few others for adjunctive evaluation. Techniques that enable mass level screening should be cost-effective and efficient enough to reach the masses. Once breast cancer has been detected in screening tests, more detailed evaluations are usually performed using diagnostic modalities which may also be used for initial diagnosis. Adjunctive modalities are used to provide the doctors and clinicians with additional confidence in their initial diagnosis. The currently used modalities include mammography, breast ultrasound, thermography, magnetic resonance imaging (MRI), positron emission tomography (PET), scintimammography, optical imaging, electrical impedance based imaging, and computed tomography (CT).

Since cancer is a complex disease with varied pathology, many variations of the basic detection technique used in each of these modalities have been carried out over the years in order to improve the detection efficiency^[8]. The main aim of this paper is to provide a discussion on the capabilities of each of these modalities, which are presented in the following sections.

VARIOUS MODALITIES USED FOR BREAST CANCER DETECTION

This section presents a review of the various modalities used for breast cancer detection.

Mammography

Mammography is the most common method of breast imaging. It uses low-dose amplitude-X-rays to examine the human breast. Cancerous masses and calcium deposits appear brighter on the mammogram. This method is good for detecting Ductal Carcinoma In Situ (DCIS) and calcifications. Currently, mammography is the gold standard method to detect early stage breast cancer before the lesions become clinically palpable. Mammography has helped to decrease the mortality rate by 25%-30% in screened women when compared with a control group after 5 to 7 years^[9]. Randomized trials of mammographic screening have provided strong evidence that early diagnosis and treatment of breast cancer reduces breast cancer mortality^[10].

It is very difficult to detect cancer in the early stage using mammographic screening. However, additional screening tests may reduce the death rate from breast cancer. The mammography screening test has been shown to lower the death rate in randomized controlled trials conducted with the general population^[11-13]. Mammographic imaging has proved to be scientifically more suitable for screening, and hence, may be used for general screening^[12]. Patients with abnormal breast findings were screened using mammography, sonography and magnetic resonance (MR) mammography^[14]. Carcinoma *in situ* was diagnosed in 78.9%

and 68.4% of patients using mammography and MR mammography, respectively. A combination of all three diagnostic methods performed better in detecting invasive cancer and multifocal disease. However, the sensitivity of mammography and sonography combined was identical to the performance of MR mammography (i.e. 94.6%).

In digital tomosynthesis mammography, the basic mammography technique has been modified to acquire 3D views of the breast^[15]. In another variation called ductography, contrast agents are used to determine the presence of a mass within the ducts. A recent development of mammography is contrast-enhanced digital mammography (CEDM) which uses an intravenous injection of an iodinated contrast agent in conjunction with a mammography examination^[16]. Diekmann *et al*^[17] evaluated the diagnostic benefits of CEDM over conventional mammography. They found an increase in sensitivity from 0.43 to 0.62 on using CEDM, and also observed better sensitivity in the case of dense tissues. This is a potentially useful benefit as it is known that conventional mammography is not very sensitive in detecting cancer in dense breast tissues.

Breast ultrasound

Ultrasound imaging is used to detect breast lesions and it is used as an adjunct tool for detecting the location of the suspicious lesion. The ultrasound transducer directs high-frequency sound waves into the breast tissues and detects the reflected sound waves. These detected waves are used to display 2D images. As the sensor is moved over the breast, continuous real-time images can be captured. Ultrasound can be used as an adjunct to mammography for clinical examination in the assessment of both palpable and impalpable breast abnormalities. Ultrasound screening in asymptomatic women causes unacceptable false positive and false negative outcomes^[18]. Hence, there is little evidence to support the use of breast ultrasound in breast cancer screening.

Mammography alone misses many cancers in dense-breasted women. The diagnostic yield of mammography with an automated whole breast ultrasound (AWBU), for women with dense breasts and/or at elevated risk of breast cancer, is better^[19]. A study by Kelly *et al*^[19] showed that 87% of cancer detections added by AWBU were found in the 68% of studies in women with dense/very dense breasts. Hence, AWBU resulted in significant cancer detection improvement compared with mammography alone. Kopans^[12] has suggested that sonography should always be used with mammography or other imaging techniques. It alone will not be able to detect lesions accurately. Another study that supports the use of mammography and ultrasound together is the ACRIN 6666 trial. The results of this study indicated that incorporating a screening ultrasound with mammography would detect an additional 1.1 to 7.2 cancers per 1000 high-risk women, however, at the expense of an increased false positive rate^[20]. Breast cancer is common among Japanese women in their late 40s with small and dense breasts. It was shown that the performance of ultrasound was similar to

that of mammography in detecting breast cancers in these women^[21]. The authors of this study have also suggested that the combination of mammography and ultrasound is a suitable method for breast screening in Japan. A very recent specific study which was conducted to evaluate the efficiency of whole breast ultrasound based on BI-RADS final assessment categories in women with mammographically negative dense breasts^[22] has reported that ultrasound is useful for dense breast evaluations.

Advancements in ultrasound technology include 3D ultrasound that formats the sound wave data into 3D images^[23], automated ultrasound for a good overall view of the breast^[24], Doppler Ultrasound^[25], and sonoelastography^[26].

Breast thermography

Cancerous and pre-cancerous tissues have a higher metabolic rate resulting in growth of new blood vessels supplying nutrients to the fast growing cancer cells. As a consequence, the temperature of the area surrounding the pre-cancerous and cancerous breast tissue is higher when compared to the normal breast tissue temperature. The breast has been recognized to exhibit a circadian rhythm, which reflects the physiology. There is evidence to indicate that these rhythms, associated with malignant cell proliferation, are non-circadian^[27,28]. The relationship between breast skin temperature and breast cancer has been examined^[29,30]. Measurable changes were observed in skin temperatures between clinically healthy and cancerous breasts. The cyclic variation in temperature and vascularization of the normal breast thermograms under a controlled environment were studied^[31]. The results of this study help in the analysis of normal and abnormal breast thermography.

Nowadays, breast thermograms are widely used for the accurate detection of breast cancer^[32-38]. Thermography is a promising screening tool because it is able to diagnose breast cancer at least ten years in advance. However, both analysis and interpretation of thermograms depends on analysts.

MRI

MRI uses the hydrogen nucleus (single proton) for imaging purposes because this nucleus is abundant in water and fat. The magnetic property of the hydrogen nucleus is used to produce detailed images from any part of the body. The patient who is examined using MRI is placed in a magnetic field and a radio frequency wave is applied to create high contrast images of the breast. In dynamic contrast enhanced-MRI (DCE-MRI)^[39], a contrast agent is injected before the images are captured. This technique has been found to be more sensitive than mammography^[40].

Application of state-of-the-art imaging modalities, namely MRI, magnetic resonance spectroscopy (MRS), nuclear imaging, and optical imaging, for precise identification of human breast tumors and their use in monitoring chemotherapeutic responses has been discussed^[41]. MRI helps in investigating vascular changes associated with neoangiogenesis^[42]. It is popular in diagnosis, and is now being used to assess tumor response to treatment. It is

predicted that new contrast agents and improvements in measurement and analytical methods will help the use of MRI in investigating the vascular dependence of tumor growth and the activity of vascular-directed therapies.

Breast MRI is a widely used imaging modality for the early detection of breast cancer^[43]. Early results suggest that MRI can dramatically improve the yield of screening certain at-risk populations. Further work may be performed to clarify the role of breast MRI in the early detection of breast cancer. Recent work on breast MRI with 3 Tesla magnets, showed that MRI had a higher spatial and temporal resolution and a better signal to noise ratio^[44].

Numerous studies have demonstrated that malignant tissues have elevated levels of choline-containing compounds, suggesting that these compounds may serve as non-invasive markers for detecting malignancies^[45]. *In vivo* non-invasive MRSI uses equipment that is almost identical to the normal MRI apparatus but with specific sequences for spectroscopic signal acquisition to visualize the total choline content in the breast. MRS improves the specificity of MRI further, and it can predict response to therapy and/or evaluate very early response to chemotherapy. In a study using MRS, the specificity was observed to be 87.5% which was significantly higher than that obtained using MRI (62.5%)^[46]. Novel contrast agents are being developed to provide more sensitive and more specific discrimination of benign from malignant lesions. MRS and MRI are rapidly becoming standard capabilities of clinical MR systems with magnets 1.5 Tesla or stronger^[47]. The promising results from multiple institutions reported so far suggest that MRS, along with MRI, can improve the clinical assessment of breast cancer in the future. Numerous multicenter trials may still be needed before these new techniques can be widely used to guide diagnostic decisions and to predict response to therapy. Brain and prostate cancers also exhibit increased choline levels, and hence, MRS is suitable for assessing these cancers^[48].

In another version of MRI, namely diffusion weighted imaging (DWI), image contrast arising out of the differences in the motion of water molecules between tissues is utilized for imaging. No external contrast agents are needed. The Apparent Diffusion Constant (ADC) parameter was found to be higher in tumor tissues compared to normal tissues, and hence, this ADC has been used in the assessment of metastatic breast cancer response to chemoembolization^[49]. DWI-MRI has also been used for evaluating a variety of other cancers including liver, prostate and pancreatic carcinomas^[48].

In MRI based elastography, a periodic motion is generated by a mechanical shaker to one side of the breast and the resulting displacement field inside the breast is captured by MRI to determine the elasticity parameters^[50]. This technique relies on MRI's ability to detect slight motion. MRE studies have also been tried to assess prostate cancers^[48].

MRI is useful for women with a higher risk of breast cancer, has good image resolution, is effective for evaluating dense breasts, helps to evaluate inverted nipple, allows the simultaneous evaluation of both breasts, helps to de-

termine whether lumpectomy or mastectomy is the best treatment, and it has no side effects as there is no radiation^[51]. The limitations of this technique are that it is not good at diagnosing ductal carcinoma *in situ* (DCIS), may lead to many false positives, is slow (30 min to one hour), more expensive, and may not show all calcifications. Recently, an analysis was conducted to study the correlation between film mammography and MRI in screening breast cancer in high-risk women^[52]. The authors found no significant correlation, and suggested that using both modalities for screening is likely to improve the odds of detecting early stage cancers.

Positron emission tomography

Positron emission tomography (PET) is a nuclear medicine imaging technique which is used to produce three dimensional images. It detects a pair of γ rays, which are emitted from the radionuclide that is introduced into the human body. Malignant tumors are characterized by increased glucose metabolism compared with normal cells. This produces a good contrast between cancerous and normal cells in PET images. It provides information about the chemical functions inside organs and tissues. However, PET is very expensive and yields poor resolution images. Furthermore, the patient is subjected to radiation exposure. PET has been used frequently to predict treatment response in several cancers^[48].

Single photon emission computed tomography (SPECT) and PET use radiolabeled isotopes^[53]. Both imaging modalities provide unique opportunities to study animal models of breast cancer with direct application to human imaging. MRI and PET are complementary and valuable in monitoring response and assessing residual disease of locally advanced breast cancer treated with neoadjuvant chemotherapy^[54]. Their study suggested that the combined use of MRI and PET were complementary and offered advantages over clinical breast examination. PET was more accurate in predicting pathologic non-response, and the response evaluated using MRI correlated well with macroscopic pathologic complete response.

Scintimammography (SMM), SPECT and PET can be used as adjunct imaging tools for detecting and staging breast cancer, however, they cannot replace invasive procedures, due to insufficient sensitivity to detect small (less than 1 cm) tumor deposits^[55]. SMM is useful for assessing palpable breast masses in women with dense breasts. Several enzymes and receptors have been targeted for imaging breast cancers with PET. Fluorodeoxyglucose is useful in the detection and staging of recurrent breast cancer and assessing its response to chemotherapy.

PET used to complement mammography is known as positron emission mammography (PEM), and it has been reported that PEM may not be adversely affected by breast density, hormone replacement therapy, and menopausal status of the patient^[56].

Scintimammography

The scintimammography imaging technique uses a radioisotope to visualize lesions of the breast. It is difficult to

detect breast cancer in dense breast tissue using mammography. As a result, mammogram-based breast cancer detection techniques yield a high number of false positives. Scintimammography with technetium tetrofosmin (Tc-99 tetrofosmin) provides better precision in the diagnosis of women with dense breasts. It is suitable for dense breasts, can image breasts with implants, can image large and palpable abnormalities, and it can be used when multiple tumors are suspected^[57]. A high-resolution breast-specific gamma camera was used to evaluate the occult breast cancer in women at high risk of breast cancer^[58]. The authors found that high-resolution breast-specific scintimammography was able to detect small (< 1 cm), mammographically occult, nonpalpable lesions not otherwise detected by mammography or physical examination in women with increased risk for breast cancer. The joint use of mammography and 99mTc-methoxy isobutyl isonitrile (MIBI) scintimammography to reduce the number of biopsies required in patients with suspected breast cancer has been studied^[59]. The total number of biopsies performed was reduced by 34%. In scintimammography with Tc99m compounds, the value of planar Tc99m sestamibi scanning for auxiliary lymph node evaluation was presented^[60]. Their work confirmed that non-tomographic Tc99m sestamibi scintimammography had a very low detection rate for auxiliary lymph node involvement and may not be suitable for clinical assessment of breast cancer. The sensitivity and specificity of Breast-Specific Gamma Imaging (BSGI) for the detection of breast cancer by using pathologic results as the reference standard was determined^[61]. BSGI showed high sensitivity (96.4%) and moderate specificity (59.5%) in the detection of breast cancers.

Optical imaging

Optical imaging uses near infrared (NIR) wavelength light to detect lesions inside the breast. Diffuse optical imaging (uses NIR light to penetrate into the breast), diffuse optical tomography (uses NIR light of wavelength 700 to 1000 nm), and optical mammography (uses laser light) are the different types of optical imaging which use different wavelengths of light to detect breast lesions.

Diffuse optical imaging (DOI) is a noninvasive optical technique which uses NIR light to quantitatively characterize the properties of thick tissues^[62]. Factors affecting the DOI performance are intrinsic and extrinsic contrast mechanisms, quantitation of biochemical components, and image formation/visualization. Currently, the new direction is to develop standardized DOI platforms that can be used as stand-alone devices or in conjunction with MRI, mammography, or ultrasound which can provide new insights for detecting disease in mammographically dense tissue, distinguishing between malignant and benign lesions, and understanding the impact of neoadjuvant chemotherapies.

Optical imaging offers complementary features to radiologic imaging techniques, primarily the quantitative imaging of hemoglobin saturation and concentration, and the selective imaging of specific gene expression with high sensitivity, because background signals can be suppressed using enzyme-activated fluorescence probes^[63]. This meth-

od can also characterize vascularization, permeability, and a plethora of contrast agents with high sensitivity, without using harmful radiation, and probably at less cost.

Electrical impedance based imaging

Our body tissues offer impedance to the flow of electric current. Studies have shown that cancerous breast tissues have lower impedance when compared to normal tissues. Electrical impedance tomography (EIT) and electrical impedance scanning (EIS) are the two types of electrical impedance based imaging techniques available. In EIT, 2D or 3D images are reconstructed from a large number of impedance values which are captured by placing electrodes around the breast surface in a circular fashion. However, in EIS or electrical impedance mapping (EIM), a planar electrode array is used and there is no need for complicated reconstruction algorithms which are used for EIT.

Zou *et al.*^[64] presented a review of the noninvasive impedance imaging techniques for breast cancer detection, such as EIT and EIM. They suggested that an invasive impedance technique can be more effective by combining it with other cancer indicators. They have proposed the possibility of improving EIM using a pair of electrode arrays, one for exciting the breast surface and the other for measuring the impedance. They concluded that magnetic induction tomography and other magnetic induction based impedance imaging techniques are promising. The T-SCANTM technology and its use as a diagnostic tool for breast cancer detection was discussed by Assenheimer *et al.*^[65]. They used theoretical models with simplified geometries to show that the display of planar two-dimensional maps of the currents detected at the breast's surface related to the electric field distribution within the breast. The differences in the distribution of the various tissue types can be used to discriminate between various pathological states. They also suggested that low frequency impedance measurements can be used in breast cancer diagnosis. EIS has been found to provide a rather high sensitivity for the verification of suspicious breast lesions^[66].

The possibilities of using electrical impedance mammography for the investigation of mammary gland state in women with different hormonal status was studied^[67]. They found that electrical impedance mammograms from different groups had clear visual distinctions and statistically significant differences in mammary gland conductivity. Further investigations on histomorphological characteristics of false negative and false positive lesions may be needed to gain further knowledge about the bioelectric characteristics of breast lesions.

CT

CT uses X-rays to capture 2D images or slices of the examined body parts. Subsequently, different algorithms are used to generate corresponding 3D images which provide anatomical information such as the location of lesions. Usually CT has low contrast, and hence, iodinated contrast media is injected intravenously to increase the contrast of the CT images. The iodine contrast injection dramatically enhances the visualization of tumors. The diagnostic accuracy of CT perfusion in differentiating metastatic from

inflammatory enlarged axillary lymph nodes in patients with breast cancer was evaluated^[68]. They showed that CT perfusion may be an effective tool for studying enlarged axillary lymph nodes in patients with breast cancer. The study presents information on vascularization of lymph nodes, helping to understand the changes occurring when neoplastic cells implant in lymph nodes. The lifetime attributable risk (LAR) of cancer incidence associated with radiation exposure from 64-slice computed tomography coronary angiography (CTCA) was studied and the influence of age, sex, and scan protocol on cancer risk was evaluated^[69]. These estimates, which were derived from simulation models, suggest that the use of 64-slice CTCA was associated with a non-negligible LAR of cancer. This risk varies markedly and was considerably greater for women, younger patients, and for combined cardiac and aortic scans.

A hybrid technique combining PET and CT is useful for staging potential metastatic cancers^[70]. This technique has the combined advantages of both CT and PET: tumor location is better captured by CT and PET indicates a metabolically active or malignant tumor based on glucose uptake. CT often incidentally identifies lung nodules during exams for other lesions in the thorax. Therefore, recently, a dedicated breast CT prototype that has a high-resolution, isotropic, rotating detector was developed. Subjective evaluation of breast CT images revealed excellent anatomical detail, good depiction of microcalcifications, and exquisite visualization of soft tissue components which belong to the tumor when contrasted against adipose tissues^[71].

BIOMARKERS

A disease cannot be easily and straight-forwardly diagnosed based on symptoms as the initial symptoms may point to a group of diseases with similar features. Moreover, in the case of cancer, it will be too late to make a diagnosis based on symptoms, as symptoms appear when the tumor is relatively large. Therefore, for early detection, the modality must be capable of detecting cancer in asymptomatic women. By the time a tumor is detected by most of the current imaging modalities, molecular changes would have already occurred in the suspected area. Detection of such molecular changes, therefore, would be our best bet to capture the presence of cancer at its earliest stages. A biomarker is a measurable phenotypic parameter that characterizes an organism's state of health or disease, or a response to a particular therapeutic intervention^[72]. Diagnostic assays using such biomarkers have good potential in early cancer detection.

Studies have demonstrated the utility of direct examination of the cytomorphology of exfoliated cells in detecting breast cancer^[73]. The molecular analysis of tumor biomarkers in nipple aspirate fluid (NAF) or in ductal lavage has also been found to be useful for the detection of breast cancer^[74]. However, the cytomorphology-based analysis is subjective, and most women may not produce NAF. Lipids, carbohydrates, polyamines, proteins, and nucleic acids have also been studied as potential biomarkers for early breast

cancer detection. A detailed review of the biomarkers used for early detection can be found in^[75]

Response to therapy is first observed at the molecular and cellular level and then at the anatomical level. Therefore, biomarkers are useful in predicting treatment response. In current clinical practice, the standard markers used for general prognosis assessment and the prediction of therapy response are the hormone receptor (ER and PR) status, HER-2/neu status, and the labeling of Ki-67 antigen.

ER and PR testing have been used as markers for the prognosis and the prediction of response to anti-estrogen therapy^[76-77]. The HER2/neu is a protein that has higher aggressiveness in breast cancers. Amplification of the *HER2/neu* gene and over-expression of the HER2/neu protein have been observed in 10%-34% of invasive breast cancers^[78]. The human Ki-67 protein expression is associated with cell proliferation. The Ki-67 labeling index, which is a fraction of Ki-67-positive tumor cells, is often correlated with the clinical course of cancer. A detailed review of the emerging biomarkers used for breast cancer management (prognosis and treatment response prediction) has been carried out by Ross *et al.*^[79].

The term molecular imaging was defined by the Commission on Molecular Imaging of the American College of Radiology as “the spatially localized and/or temporally resolved sensing of molecular and cellular processes *in vivo*.” Molecular imaging explores either changes in metabolic rate, cell proliferation rate, hormone expression, gene expression, or protein production. The main modalities for molecular imaging are PET, SPECT, MRS, and optical imaging; PET imaging being the most widely used modality. PET has been used for the *in vivo* quantification of ER. Since [18F]-16 α -[fluororestradiol] (FES) has shown most promise in quantifying the functional ER status of breast cancer, it has been used as a tracer in PET-ER imaging^[80]. PET-ER imaging (FES-PET) can therefore predict the likelihood of a patient’s response to hormonal therapy, and thereby, determine the suitability of the patient for this type of treatment. The results of some related studies can be found in^[81]. Jeraj *et al.*^[82] have presented a comprehensive review of the various functional and molecular imaging techniques used in oncology. They have presented the effectiveness of such imaging techniques for a variety of cancers.

CONCLUSION

Current breast imaging modalities play a vital role in assisting clinicians in the primary screening of cancer, in the diagnosis and characterization of lesions, staging and restaging, treatment selection and treatment progress monitoring and in determining cancer recurrence. In this paper, we have discussed the capabilities of the different breast imaging techniques that are currently used in clinical setups. It is evident from the material presented in this paper that no single modality is completely useful in all areas of breast cancer management. Therefore, research is continually being carried out to improve the existing modalities and develop new modalities based on the physical,

chemical, and biological properties of cancerous breast tissue that differentiates it from normal and benign tissues. Cancer is a disease with no specific cure, and its treatment involves a wide variety of side-effects. Moreover, the survival rate is largely dependent on early detection. A disease with such disturbing and life-threatening factors warrants a huge amount of research to develop modalities (screening, diagnostic, adjunct, standalone, and hybrid) that help in early detection and in finding a possible cure. Currently, research on modality development is moving towards imaging at the molecular level. This type of imaging will also help in understanding the nature of cancer growth and development which in turn might lead us closer to finding a possible cure for this disease. Moreover, the use of computer-aided diagnosis techniques has been widely advocated for the improvement of cancer detection efficiency and for reducing the inter-observer variability that is associated with the subjective human interpretation of the images obtained.

REFERENCES

- 1 WHO IARC, World Health Organization International Agency for Research on Cancer, 2008. Available from: URL: <http://globocan.iarc.fr/factsheets/populations/factsheet.asp?uno=900>
- 2 WHO Fact sheet N°297, 2009. Available from: URL: <http://www.who.int/mediacentre/factsheets/fs297/en/index.html>
- 3 NBCF, National Breast Cancer Foundation, Inc., 2010. Available from: URL: <http://www.nationalbreastcancer.org/about-breast-cancer/what-is-breast-cancer.aspx>
- 4 Altekruse SF, Kosary CL, Krapcho M, Neyman N, Aminou R, Waldron W, Ruhl J, Howlander N, Tatalovich Z, Cho H, Mariotto A, Eisner MP, Lewis DR, Cronin K, Chen HS, Feuer EJ, Stinchcomb DG, Edwards BK, editors. SEER Cancer Statistics Review, 1975-2007, National Cancer Institute. Bethesda, MD, 2010. Available from: URL: http://seer.cancer.gov/csr/1975_2007/
- 5 Breast cancer in men, Cancer Research UK. Available from: URL: <http://www.cancerhelp.org.uk/type/breast-cancer/about/types/breast-cancer-in-men>
- 6 Male breast cancer treatment, National Cancer Institute. Available from: URL: <http://www.cancer.gov/cancertopics/pdq/treatment/malebreast/Patient>
- 7 Breast cancer in men, American Cancer Society. Available from: URL: <http://www.cancer.org/Cancer/BreastCancerinMen/DetailedGuide/breast-cancer-in-men-key-statistics>
- 8 Vinitha Sree S, Ng EYK, Rajendra Acharya U, William Tan. Breast imaging systems: a review and comparative study. *J Mech Med Biol* 2010; **10**: 5-34
- 9 Kerlikowske K, Grady D, Rubin SM, Sandrock C, Ernster VL. Efficacy of screening mammography. A meta-analysis. *JAMA* 1995; **273**: 149-154
- 10 Nyström L, Andersson I, Bjurstram N, Frisell J, Nordenskjöld B, Rutqvist LE. Long-term effects of mammography screening: updated overview of the Swedish randomised trials. *Lancet* 2002; **359**: 909-919
- 11 Kopans DB. Beyond randomized controlled trials: organized mammographic screening substantially reduces breast carcinoma mortality. *Cancer* 2002; **94**: 580-581; author reply 581-583
- 12 Kopans DB. Sonography should not be used for breast cancer screening until its efficacy has been proven scientifically. *AJR Am J Roentgenol* 2004; **182**: 489-491
- 13 Tabar L, Yen MF, Vitak B, Chen HH, Smith RA, Duffy SW.

- Mammography service screening and mortality in breast cancer patients: 20-year follow-up before and after introduction of screening. *Lancet* 2003; **361**: 1405-1410
- 14 **Malur S**, Wurdinger S, Moritz A, Michels W, Schneider A. Comparison of written reports of mammography, sonography and magnetic resonance mammography for preoperative evaluation of breast lesions, with special emphasis on magnetic resonance mammography. *Breast Cancer Res* 2001; **3**: 55-60
 - 15 **Wu T**, Stewart A, Stanton M, McCauley T, Phillips W, Kopans DB, Moore RH, Eberhard JW, Opsahl-Ong B, Niklason L, Williams MB. Tomographic mammography using a limited number of low-dose cone-beam projection images. *Med Phys* 2003; **30**: 365-380
 - 16 **Dromain C**, Balleyguier C, Adler G, Garbay JR, Delaloue S. Contrast-enhanced digital mammography. *Eur J Radiol* 2009; **69**: 34-42
 - 17 **Diekmann F**, Freyer M, Diekmann S, Fallenberg EM, Fischer T, Bick U, Pöllinger A. Evaluation of contrast-enhanced digital mammography. *Eur J Radiol* 2009; Epub ahead of print
 - 18 **Teh W**, Wilson AR. The role of ultrasound in breast cancer screening. A consensus statement by the European Group for Breast Cancer Screening. *Eur J Cancer* 1998; **34**: 449-450
 - 19 **Kelly KM**, Dean J, Comulada WS, Lee SJ. Breast cancer detection using automated whole breast ultrasound and mammography in radiographically dense breasts. *Eur Radiol* 2010; **20**: 734-742
 - 20 **Berg WA**, Blume JD, Cormack JB, Mendelson EB, Lehrer D, Böhm-Vélez M, Pisano ED, Jong RA, Evans WP, Morton MJ, Mahoney MC, Larsen LH, Barr RG, Farria DM, Marques HS, Boparai K. Combined screening with ultrasound and mammography vs mammography alone in women at elevated risk of breast cancer. *JAMA* 2008; **299**: 2151-2163
 - 21 **Tohno E**, Ueno E, Watanabe H. Ultrasound screening of breast cancer. *Breast Cancer* 2009; **16**: 18-22
 - 22 **Youk JH**, Kim EK, Kim MJ, Kwak JY, Son EJ. Performance of hand-held whole-breast ultrasound based on BI-RADS in women with mammographically negative dense breast. *Eur Radiol* 2011; **21**: 667-675
 - 23 **Carsten Riis C**, Lernevall A, Sorensen FB, Nygaard H. 3D Ultrasound-based evaluation of lesions in the uncompressed breast. In: Ueno E, Shiina T, Kubota M, Sawai K, editors. Research and Development in Breast Ultrasound. Tokyo: Springer, 2005: 151-155
 - 24 **TechniScan**. Svara™ Warm Bath Ultrasound (WBU™) Imaging System. Available from: URL: <http://www.techniscanmedicalsystems.com/index.php?p=Home>
 - 25 **Kook SH**, Park HW, Lee YR, Lee YU, Pae WK, Park YL. Evaluation of solid breast lesions with power Doppler sonography. *J Clin Ultrasound* 1999; **27**: 231-237
 - 26 **Scaperrotta G**, Ferranti C, Costa C, Mariani L, Marchesini M, Suman L, Folini C, Bergonzi S. Role of sonoelastography in non-palpable breast lesions. *Eur Radiol* 2008; **18**: 2381-2389
 - 27 **Keith LG**, Oleszczuk JJ, Laguens M. Circadian rhythm chaos: a new breast cancer marker. *Int J Fertil Womens Med* 2001; **46**: 238-247
 - 28 **Salhab M**, Sarakbi WAI, Mokbel K. The evolving role of the dynamic thermal analysis in the early detection of breast cancer. *Int Semin Surg Oncol* 2005; **2**: 8. Available from: URL: <http://www.issonline.com/content/2/1/8>
 - 29 **Gauthierine M**, Gros C. Contribution of infrared thermography to early diagnosis, pretherapeutic prognosis and post-irradiation follow-up of breast carcinomas. *Med Mundi* 1976; **21**: 135-149
 - 30 **Gros C**, Gauthierine M, Bourjat P. Prognosis and post-therapeutic follow-up of breast cancers by thermography. *Bibl Radiol* 1975; :77-90
 - 31 **Ng EYK**, Chen Y, Ung LN. Computerized breast thermography: study of image segmentation and temperature cyclic variations. *Int J Med Eng Technol* 2001; **25**: 12-16
 - 32 **Ng EYK**. A review of thermography as promising non-invasive detection modality for breast tumour. *Int J Therm Sci* 2009; **48**: 849-859
 - 33 **Ng EYK**, Sudharsan NM. Numerical modeling in conjunction with thermography as an adjunct tool for breast tumour detection. *BMC Cancer* 2004; **4**: 1-26
 - 34 **Ammer K**, Ring EFJ. Standard procedures for infrared imaging in medicine. In: Biomedical Engineering Handbook. CRC Press, 2006: chapter 36: 1-14
 - 35 **Amalu WC**, Hobbins WB, Head JF, Elliott RL. Infrared imaging of the breast - an overview. In: Biomedical Engineering Handbook. CRC Press, 2006: chapter 25: 1-36
 - 36 **Wiecek B**, Wiecek M, Strakowski R, Jakubowska T, Ng EYK. Wavelet-based thermal image classification for breast screening and other medical applications. In: Ng EYK, Acharya RU, Suri JS. Performance Evaluation Techniques in Multimodality Breast Cancer Screening, Diagnosis and Treatment. American Scientific Publishers, 2010
 - 37 **Qi H**, Kuruganti PT, Snyder WE. Detecting breast cancer from thermal infrared images by asymmetry analysis. In: Biomedical Engineering Handbook. CRC Press, 2006: chapter 27: 1-14
 - 38 **Ring EFJ**, Ammer K. The technique of infra red imaging in medicine. *Thermology Int* 2000; **10**: 7-14
 - 39 **Heywang-Köbrunner SH**, Viehweg P, Heinig A, Küchler C. Contrast-enhanced MRI of the breast: accuracy, value, controversies, solutions. *Eur J Radiol* 1997; **24**: 94-108
 - 40 **Liu PF**, Debatin JF, Caduff RF, Kacl G, Garzoli E, Krestin GP. Improved diagnostic accuracy in dynamic contrast enhanced MRI of the breast by combined quantitative and qualitative analysis. *Br J Radiol* 1998; **71**: 501-509
 - 41 **Basilion JP**. Current and future technologies for breast cancer imaging. *Breast Cancer Res* 2001; **3**: 14-16
 - 42 **Leach MO**. Application of magnetic resonance imaging to angiogenesis in breast cancer. *Breast Cancer Res* 2001; **3**: 22-27
 - 43 **Schnall MD**. Application of magnetic resonance imaging to early detection of breast cancer. *Breast Cancer Res* 2001; **3**: 17-21
 - 44 **Lehman CD**, Schnall MD. Imaging in breast cancer: Magnetic resonance imaging. *Breast Cancer Res* 2005; **7**: 215-219
 - 45 **Meisamy S**, Bolan PJ, Garwood M. Magnetic resonance spectroscopy of breast cancer: current techniques and clinical applications. In: Hayat MA, editor. Lung and breast carcinomas. Elsevier, 2008: 407-415
 - 46 **Huang W**, Fisher PR, Dulaimy K, Tudorica LA, O'Hea B, Button TM. Detection of breast malignancy: diagnostic MR protocol for improved specificity. *Radiology* 2004; **232**: 585-591
 - 47 **Bolan BJ**, Nelson MT, Yee D, Garwood M. Imaging in breast cancer: Magnetic resonance spectroscopy of the breast. *Breast Cancer Res* 2005; **7**: 149-152
 - 48 **Fass L**. Imaging and cancer: a review. *Mol Oncol* 2008; **2**: 115-152
 - 49 **Buijs M**, Kamel IR, Vossen JA, Georgiades CS, Hong K, Geschwind JF. Assessment of metastatic breast cancer response to chemoembolization with contrast agent enhanced and diffusion-weighted MR imaging. *J Vasc Interv Radiol* 2007; **18**: 957-963
 - 50 **Van Houten EE**, Doyley MM, Kennedy FE, Weaver JB, Paulsen KD. Initial in vivo experience with steady-state subzone-based MR elastography of the human breast. *J Magn Reson Imaging* 2003; **17**: 72-85
 - 51 **Stephan P**. Mammography and Breast MRIs. 2010. Available from: URL: http://breastcancer.about.com/od/mammograms/a/mammo_vs_mri_2.htm
 - 52 **Lee JM**, Halpern EF, Rafferty EA, Gazelle GS. Evaluating the correlation between film mammography and MRI for screening women with increased breast cancer risk. *Acad Radiol* 2009; **16**: 1323-1328
 - 53 **Berger F**, Gambhir SS. Recent advances in imaging endogenous or transferred gene expression utilizing radionuclide technologies in living subjects: applications to breast cancer. *Breast Cancer Res* 2001; **3**: 28-35

- 54 **Chen X**, Moore MO, Lehman CD, Mankoff DA, Lawton TJ, Peacock S, Schubert EK, Livingston RB. Combined use of MRI and PET to monitor response and assess residual disease for locally advanced breast cancer treated with neoadjuvant chemotherapy. *Acad Radiol* 2004; **11**: 1115-1124
- 55 **Benard F**, Turcotte E. Imaging breast cancer with single photon computed tomography and positron emission tomography. *Breast Cancer Res* 2005; **7**: 153-162
- 56 **Schilling K**, Narayanan D, Kalinyak JE. Effect of breast density, menopausal status, and hormone use in high resolution positron emission mammography. *Radiol Soc North Am* 2008; VB31-04
- 57 **Munshi S**. Scintimammography - an emerging technique for Breast Imaging. 2008. Available from: URL: <http://www.frost.com/prod/servlet/market-insight-top.pag?docid=137248277>
- 58 **Brem RF**, Rapelyea JA, Zisman G, Mohtashemi K, Raub J, Teal CB, Majewski S, Welch BL. Occult breast cancer: scintimammography with high-resolution breast-specific gamma camera in women at high risk for breast cancer. *Radiology* 2005; **237**: 274-280
- 59 **Prats E**, Aisa F, Abós MD, Villavieja L, García-López F, Asenjo MJ, Razola P, Banzo J. Mammography and 99mTc-MIBI scintimammography in suspected breast cancer. *J Nucl Med* 1999; **40**: 296-301
- 60 **Massardo T**, Alonso O, Llamas-Ollier A, Kabasakal L, Ravishankar U, Morales R, Delgado L, Padhy AK. Planar Tc99m-sestamibi scintimammography should be considered cautiously in the axillary evaluation of breast cancer protocols: results of an international multicenter trial. *BMC Nucl Med* 2005; **5**: 4
- 61 **Brem RF**, Floerke AC, Rapelyea JA, Teal C, Kelly T, Mathur V. Breast-specific gamma imaging as an adjunct imaging modality for the diagnosis of breast cancer. *Radiology* 2008; **247**: 651-657
- 62 **Tromberg BJ**, Pogue BW, Paulsen KD, Yodh AG, Boas DA, Cerussi AE. Assessing the future of diffuse optical imaging technologies for breast cancer management. *Med Phys* 2008; **35**: 2443-2451
- 63 **Ntziachristos V**, Chance B. Probing physiology and molecular function using optical imaging: applications to breast cancer. *Breast Cancer Res* 2001; **3**: 41-46
- 64 **Zou Y**, Guo Z. A review of electrical impedance techniques for breast cancer detection. *Med Eng Phys* 2003; **25**: 79-90
- 65 **Assenheimer M**, Laver-Moskovitz O, Malonek D, Manor D, Nahaliel U, Nitzan R, Saad A. The T-SCAN technology: electrical impedance as a diagnostic tool for breast cancer detection. *Physiol Meas* 2001; **22**: 1-8
- 66 **Malich A**, Böhm T, Facius M, Kleinteich I, Fleck M, Sauner D, Anderson R, Kaiser WA. Electrical impedance scanning as a new imaging modality in breast cancer detection—a short review of clinical value on breast application, limitations and perspectives. *Nucl Instrum Meth A* 2003; **497**: 75-81
- 67 **Cherepenin VA**, Karpov AY, Korjnevsky AV, Kornienko VN, Kultiasov YS, Ochapkin MB, Trochanova OV, Meister JD. Three-dimensional EIT imaging of breast tissues: system design and clinical testing. *IEEE Trans Med Imaging* 2002; **21**: 662-667
- 68 **Liu Y**, Bellomi M, Gatti G, Ping X. Accuracy of computed tomography perfusion in assessing metastatic involvement of enlarged axillary lymph nodes in patients with breast cancer. *Breast Cancer Res* 2007; **9**: R40
- 69 **Einstein AJ**, Henzlova MJ, Rajagopalan S. Estimating risk of cancer associated with radiation exposure from 64-slice computed tomography coronary angiography. *JAMA* 2007; **298**: 317-323
- 70 **Avril N**, Mather SJ, Roylance R. FDG-PET and PET/CT in breast cancer staging. *Breast Care* 2007; **2**: 372-377
- 71 **Boone JM**, Kwan AL, Yang K, Burkett GW, Lindfors KK, Nelson TR. Computed tomography for imaging the breast. *J Mammary Gland Biol Neoplasia* 2006; **11**: 103-111
- 72 **Negm RS**, Verma M, Srivastava S. The promise of biomarkers in cancer screening and detection. *Trends Mol Med* 2002; **8**: 288-293
- 73 **Buehring GC**. Screening for breast atypias using exfoliative cytology. *Cancer* 1979; **43**: 1788-1799
- 74 **Buehring GC**, Letscher A, McGirr KM, Khandhar S, Che LH, Nguyen CT, Hackett AJ. Presence of epithelial cells in nipple aspirate fluid is associated with subsequent breast cancer: a 25-year prospective study. *Breast Cancer Res Treat* 2006; **98**: 63-70
- 75 **Levenson VV**. Biomarkers for early detection of breast cancer: what, when, and where? *Biochim Biophys Acta* 2007; **1770**: 847-856
- 76 **Osborne CK**. Steroid hormone receptors in breast cancer management. *Breast Cancer Res Treat* 1998; **51**: 227-238
- 77 **Locker GY**. Hormonal therapy of breast cancer. *Cancer Treat Rev* 1998; **24**: 221-240
- 78 **Pusztai L**, Ayers M, Stec J, Clark E, Hess K, Stivers D, Damokosh A, Sneige N, Buchholz TA, Esteva FJ, Arun B, Cristofanilli M, Booser D, Rosales M, Valero V, Adams C, Hortobagyi GN, Symmans WF. Gene expression profiles obtained from fine-needle aspirations of breast cancer reliably identify routine prognostic markers and reveal large-scale molecular differences between estrogen-negative and estrogen-positive tumors. *Clin Cancer Res* 2003; **9**: 2406-2415
- 79 **Ross JS**, Symmans WF, Pusztai L, Hortobagyi GN. Breast cancer biomarkers. *Adv Clin Chem* 2005; **40**: 99-125
- 80 **Katzenellenbogen JA**, Welch MJ, Dehdashti F. The development of estrogen and progestin radiopharmaceuticals for imaging breast cancer. *Anticancer Res* 1997; **17**: 1573-1576
- 81 **Hospers GA**, Helmond FA, de Vries EG, Dierckx RA, de Vries EF. PET imaging of steroid receptor expression in breast and prostate cancer. *Curr Pharm Des* 2008; **14**: 3020-3032
- 82 **Jeraj R**, Meyerand ME. Molecular and functional imaging in radiation oncology. *Cancer Treat Res* 2008; **139**: 63-95

S- Editor Cheng JX L- Editor Webster JR E- Editor Ma WH

Eddie Yin-Kwee Ng, PhD, PGDTHE, Associate Professor, Series Editor

Online volume rendering of incrementally accumulated LSCEM images for superficial oral cancer detection

Wei Ming Chiew, Feng Lin, Kemao Qian, Hock Soon Seah

Wei Ming Chiew, Feng Lin, Kemao Qian, Hock Soon Seah, School of Computer Engineering, Nanyang Technological University, Singapore 639798, Singapore

Author contributions: Chiew WM, Lin F, Qian K and Seah HS performed research; Ming CW and Lin F wrote the paper.

Supported by The grant SBIC RP C-010/2006 from A*Star Biomedical Research Council

Correspondence to: Feng Lin, Associate Professor, School of Computer Engineering, Nanyang Technological University, Singapore 639798, Singapore. asflin@ntu.edu.sg

Telephone: +65-67906184 Fax: +65-67926559

Received: August 19, 2010 Revised: November 15, 2010

Accepted: November 22, 2010

Published online: April 10, 2011

Key words: Confocal endomicroscope; Field-programmable gate arrays; Incrementally accumulated volume rendering; Realtime; Online cancer detection

Peer reviewer: Brendan Curran Stack, JR, MD, FACS, FACE, Chief, McGill Family Division of Clinical Research, Department of Otolaryngology-HNS, University of Arkansas for Medical Sciences, 4301 West Markham, Slot 543, Little Rock, AR 72205, United States

Chiew WM, Lin F, Qian K, Seah HS. Online volume rendering of incrementally accumulated LSCEM images for superficial oral cancer detection. *World J Clin Oncol* 2011; 2(4): 179-186 Available from: URL: <http://www.wjgnet.com/2218-4333/full/v2/i4/179.htm> DOI: <http://dx.doi.org/10.5306/wjco.v2.i4.179>

Abstract

Laser scanning confocal endomicroscope (LSCEM) has emerged as an imaging modality which provides non-invasive, *in vivo* imaging of biological tissue on a microscopic scale. Scientific visualizations for LSCEM datasets captured by current imaging systems require these datasets to be fully acquired and brought to a separate rendering machine. To extend the features and capabilities of this modality, we propose a system which is capable of performing realtime visualization of LSCEM datasets. Using field-programmable gate arrays, our system performs three tasks in parallel: (1) automated control of dataset acquisition; (2) imaging-rendering system synchronization; and (3) realtime volume rendering of dynamic datasets. Through fusion of LSCEM imaging and volume rendering processes, acquired datasets can be visualized in realtime to provide an immediate perception of the image quality and biological conditions of the subject, further assisting in realtime cancer diagnosis. Subsequently, the imaging procedure can be improved for more accurate diagnosis and reduce the need for repeating the process due to unsatisfactory datasets.

© 2011 Baishideng. All rights reserved.

INTRODUCTION

A variety of medical imaging modalities such as computed tomography (CT) scanning^[1], ultrasound imaging^[2] and magnetic resonance imaging (MRI)^[3] are used to capture digital images of biological tissue and structures. The laser scanning confocal endomicroscope (LSCEM)^[4] is an emerging modality used to perform non-invasive, *in vivo* scanning at a microscopic scale beneath the tissue surface. This technique is also useful to capture volumetric datasets by capturing slices at progressive depth levels. The LSCEM which is an extended variation of the laser scanning confocal microscope (LSCM)^[5,6], has a miniature probe to perform *in vivo* imaging on live tissue in hard to reach areas.

Typically, LSCM is able to penetrate and section a specimen up to 50 μm or more^[7], which enables image acquisition at different depths, subsequently permitting volumetric dataset capturing. The image quality is much improved compared to other widefield microscopy techniques^[6] due to the isolation from background fluorescence signals. Furthermore, this modality enables live *in vivo* imaging^[8], minimizing patient's agony of biopsy and

avoiding flaws arising due to physical tissue cutting and specimen staining.

However, the procedural tasks for undergoing LSCEM imaging involve consumption of valuable time and resources. Firstly, current LSCEM imaging systems require manual control fully operated by the user. Secondly, the presence of typical imaging flaws such as poor dataset quality, which can only be realized after imaging ceases, will require the procedure to be re-performed. Apart from that, the lack of a realtime volume visualization system limits the flexibility for changes on-the-spot during imaging.

Performing diagnoses for diseases and medical abnormalities is a complex operation which requires trained expertise to provide an accurate outcome. However, having experienced diagnosticians alone is not enough, as the help of additional imaging and computing systems are also crucial. There has been discussion about the need for interactive visualization of LSCM datasets^[9]. Consequently, it is meaningful to explore various ideas and methods proposed to view 3D datasets as 2D images. Scientific visualization of medical datasets has always been important to aid practitioners relate changes across acquired data images and perceive them visually for more precise analyses. These relations and changes are normally difficult or impossible to realize under traditional methods of reading separate data. It is also clinically useful if the captured slices can be perceived from arbitrary viewing angles or highlight desired features. These functions introduce user interaction and further promote the effectiveness of visualization.

In view of that, we present an online visualization system which performs volume rendering on-the-fly while LSCEM imaging is being carried out. In our aim to improve the imaging procedure, this system should perform the required tasks without alterations to its pre-existing features and performances.

PREVIOUS WOKE

The LSCEM is a useful tool used to visualize microscopic tissue structures to a high level of detail. Since the advent of LSCEM for medical-based applications, many procedures have used this modality to obtain volume datasets^[4,10-11]. Further improvements on the obtained datasets involved work including image processing methods. Some of the works include deconvolution methods^[12-14] to mitigate image degradation^[15], and volume reconstruction^[16] for the misalignment problem. Recently LSCM has also been combined with reconfigurable computing to provide realtime imaging for instant diagnosis and tissue assessment^[17].

Initial attempts to visualize LSCM datasets using volume rendering is presented by Sakas *et al.*^[18]. The authors discussed methods to render LSCM datasets, including surface reconstruction^[19], maximum intensity projection (MIP)^[20], and using illumination models. A specially developed visualization system known as proteus^[21] is used to visualize time dependent LSCM data, focusing on the analysis of chromatin condensation and decondensation during mitosis. From the conducted experiments the au-

thors concluded that there was no all around visualization technique at the time of publishing, and that various techniques should be offered, each with its own strengths and weaknesses.

Fast visualization of LSCM datasets using the ray casting algorithm has shown the capability to provide interactive examination of datasets, improving the understanding of LSCM imaging. Further enhancement using pre-processing for intensity compensation and image deconvolution to enhance the dataset is also useful.

Volume rendering is the study of displaying 3D objects onto a 2D screen. A generalized rendering equation^[22] is initially used to model physical properties of light transport. This equation describes the way objects are viewed in reality, enabling computing systems to simulate these phenomena. Subsequently, this equation is used as a theoretical basis for varying model derivations^[23]. One of the most commonly used methods for rendering objects is the ray tracing algorithm. The algorithm can be used to model different objects, including polynomial surfaces^[24], fractal surfaces and shapes^[25], as well as volumetric densities^[26].

Initially, CT scanned datasets are visualized using multiplanar reconstruction^[27], which provides cross sectional representations using arbitrary configurations. The VolVis framework^[28-29] is used to visualize MRI and confocal cell imaging datasets. This system is further extended to include global illumination and shadow casting^[30]. A multidimensional transfer function^[31] is used to render the human head and brain datasets into meaningful imaging, enabling the human user to intuitively identify different tissue material and boundaries. An open source toolkit known as the medical imaging interaction toolkit (MITK)^[32], promotes interactivity and image analysis specifically for visualization of medical datasets. This system is subsequently included in the development of a software platform for medical image processing and analysis^[33], with the aim of incorporating medical image processing algorithms into a complete framework.

MATERIALS AND METHODS

Overview

The involved imaging device in our project is the Optiscan FIVE1 Endomicroscope (Optiscan Imaging Ltd., Victoria, Australia). This device is capable of scanning an area of $475 \mu\text{m} \times 475 \mu\text{m}$ with up to 1024×1024 resolution. The scanning time for each slice with the highest resolution is approximately 1.4 s. Operating the LSCEM device requires at least one person. Functional interfaces include: (1) directing the probe to the desired imaging area; (2) controlling image scanning using a footswitch control panel; and (3) managing the dataset through the imaging software on a PC.

The conventional imaging procedure on the device is commenced by applying fluorescent material to the tissue. After absorption, the tissue will emit light signals when laser light is applied. Capture trigger and imaging depth are fully operated manually by the user. To capture a full volumetric dataset, the operator has to repetitively increment depths and capture slices individually. This

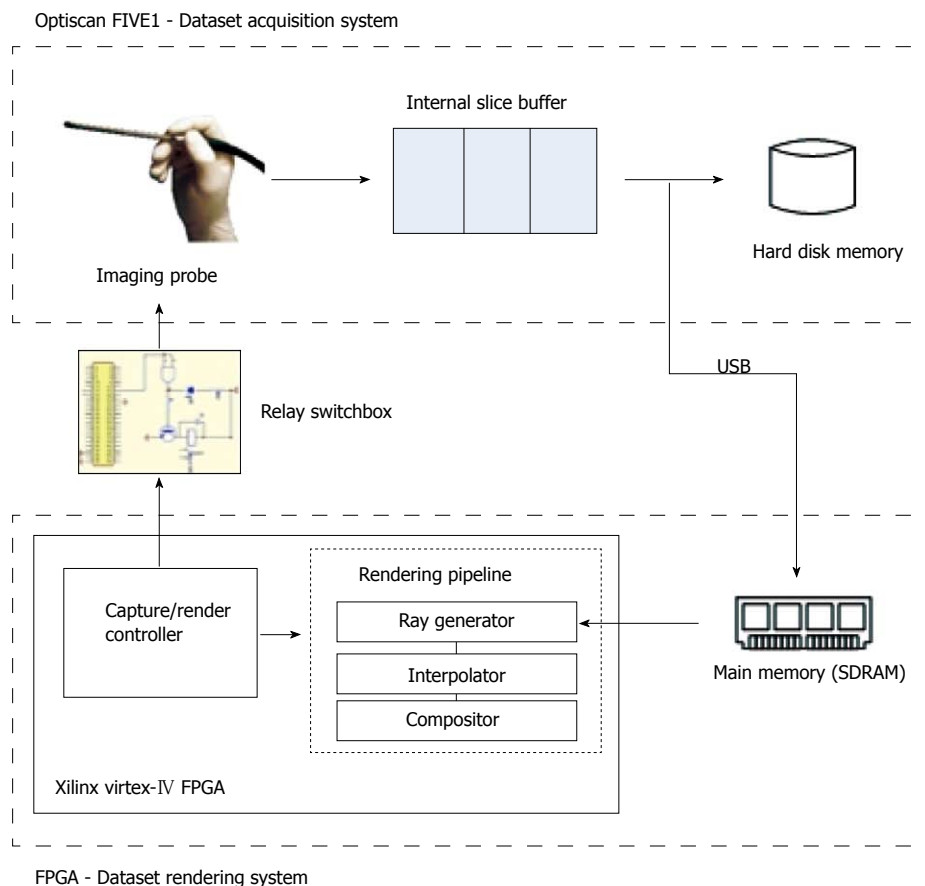


Figure 1 The system architecture.

results in a prolonged imaging session, where tissue or probe movements may be introduced to compromise the dataset accuracy. Also, such controls are tedious and repetitive, so an automated system is desired.

We built our prototype system on a field-programmable gate array (FPGA) chip. The Celoxica RC340 FPGA Development board is the main platform we use to program the FPGA. FPGAs are future oriented building bricks that allow logic circuits to be implemented in any fashion. System-on-Chip designs can thus be built on a single device using FPGAs. FPGAs are also well-known for the reconfigurable feature, which allows different designs to be implemented on the same chip. This promotes lower design costs and ease of prototyping. In our system, we integrate automated imaging control, real-time rendering and task allocation into a single device, which makes FPGAs suitable as they do not adhere to any fixed computational or programming models.

The FPGA is responsible for running three core tasks in parallel. Firstly, to efficiently couple the imaging and rendering systems reliably, task allocation and synchronization is maintained by the FPGA. Secondly, the FPGA acts as an automated controller to replace the existing footswitch for dataset acquisition. Finally, the entire volume rendering system is built on the FPGA due to support for full algorithm flexibility.

The image-ordered ray casting algorithm is used for rendering. This algorithm casts rays from each pixel on

the screen towards the dataset and is an iteration process which visits each pixel on the viewing screen. Along each ray, points of a constant distance are sampled. Finally sampling points on each ray are combined in a compositing module and the output is used as the display pixel. Various compositing methods are present, commonly MIP, averaging, nearest-point and alpha compositing.

System design

We designed the imaging-rendering system as shown in Figure 1. We developed the novel volume renderer using reconfigurable hardware for experimentation flexibility and cheaper cost for replicating prototypes. Through a handheld probe the Optiscan FIVE1 imaging device captures endoscopic images at incremental steps within the tissue depth to build up volumetric data. This is achieved by detecting the light signals emitted from the fluorescent chemical applied to the biological tissue. These signals, when captured by confining to a single focal plane, form an image slice. Consecutive slices captured across increasing depth will thus form a volume dataset.

Default operations involve using the provided footswitch for depth control, calibration and triggering the capture process. The supplied configuration requires the user to increment capture depths slice-by-slice and send instructions to manually progress to the next slice and trigger a capture. This poses disadvantages which include prolonged capture time and complications that arise, due

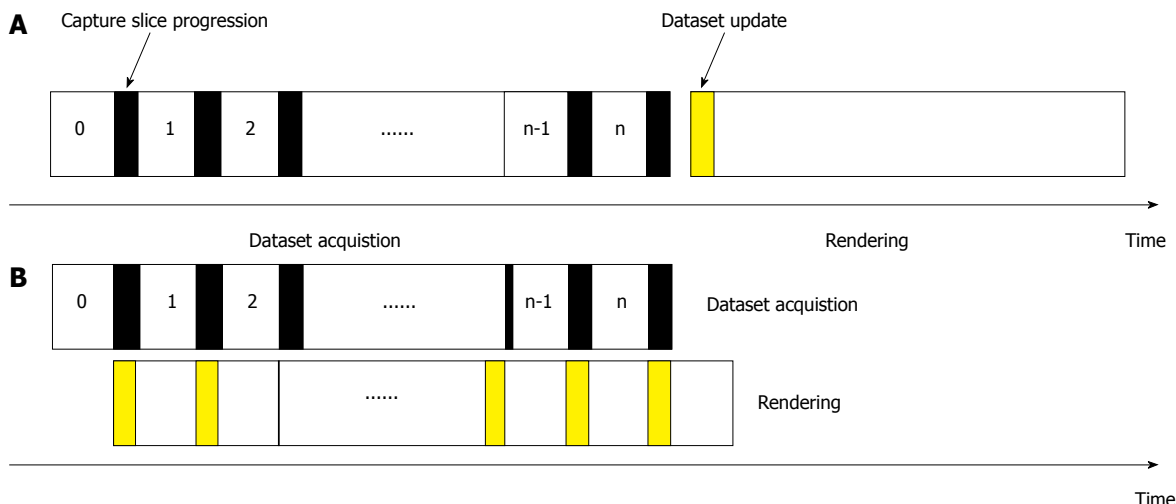


Figure 2 Imaging-rendering allocation. A: Conventional procedure; B: Simultaneous dataset capture and rendering.

to change of state and condition of the tissue. Requiring the user to hold the probe while performing stepping controls on the footswitch will introduce distortion due to movements, which is significant at a microscopic scale.

Apart from that, to perform continuous online rendering, scanning along the z-depth direction must be continuous and progress incrementally deeper into the tissue. In response, we developed an alternative hardware to substitute the footswitch^[34]. The main task of the relay switchbox hardware is to replace the manual controls of the footswitch by sending automated signals at constant intervals to increment the z-depth value every time a slice capture is complete. The user is no longer required to manually increment plane depths and initiate capture with this substitute.

For this design, the FPGA is required to fulfill the following requirements: (1) capability to perform all the rendering computations; (2) provide realtime control signals over the imaging device; and (3) support automated scanning and capturing controls.

In the LSCEM device, the captured data are buffered in an internal memory while the scanning point moves across the subject in a raster scanning fashion. We forward an entire slice after each completed capture *via* the USB to our rendering device, ensuring that the rendered result is continuously updated as soon as the slice is acquired. Once the first slice is received, rendering is initiated. An electronic controller manages the rendering and imaging tasks, so the operations of the imaging device do not affect the renderer and vice versa. Rendering is performed in conjunction with acquisition, where after each capture the relay switchbox instructs the probe to progress to the next slice automatically.

The imaging-rendering arrangement is illustrated in Figure 2. Conventional practices require the full dataset to be completed and imaging to be ceased before rendering in an alternative engine. We allocate these two processes to be performed concurrently, so that immediate results can be shown as soon as a slice is captured. The rendering and

imaging operations are performed in parallel, and the imaging always captures an additional slice to be rendered for the next cycle.

The process is initiated with a slice capture by the imaging system, while the renderer is on standby as the dataset is empty. After a complete slice is captured, it is forwarded and stored in the SDRAM of the FPGA system. Rendering proceeds by retrieving required voxels for computation from the SDRAM. The SDRAM as a shared resource between imaging and rendering must be allocated to be mutually exclusive to avoid access conflicts.

The operations repeat until the final slice as determined by the user, when capturing is ceased. Rendering can still be performed on the existing dataset until it is terminated by the user.

OPTIMIZATIONS

To accommodate for the realtime requirements of the system, we have also employed several custom designed optimizations on the FPGA rendering system.

Pre-computing ray parameters for ray casting traversal

This optimization eliminates repetitive matrix transformation computations for sampling coordinates. In this case, matrix multiplications are reduced to simple arithmetic addition and subtraction operations. The ray parameters are represented by a coordinate for the ray origin and a vector for the ray direction.

Cubic memory organization for dataset storage

We store the dataset voxels according to a customized arrangement in the SDRAM as shown in Figure 3. This is due to trilinear interpolation for sampling voxels, which requires eight memory accesses to the SDRAM. Storing dataset voxels in a cubic fashion enables fast retrieval of these points for computations in a single cycle due to the 64-bit data bus. Using this technique, sampling points require less memory access for more efficient operations.

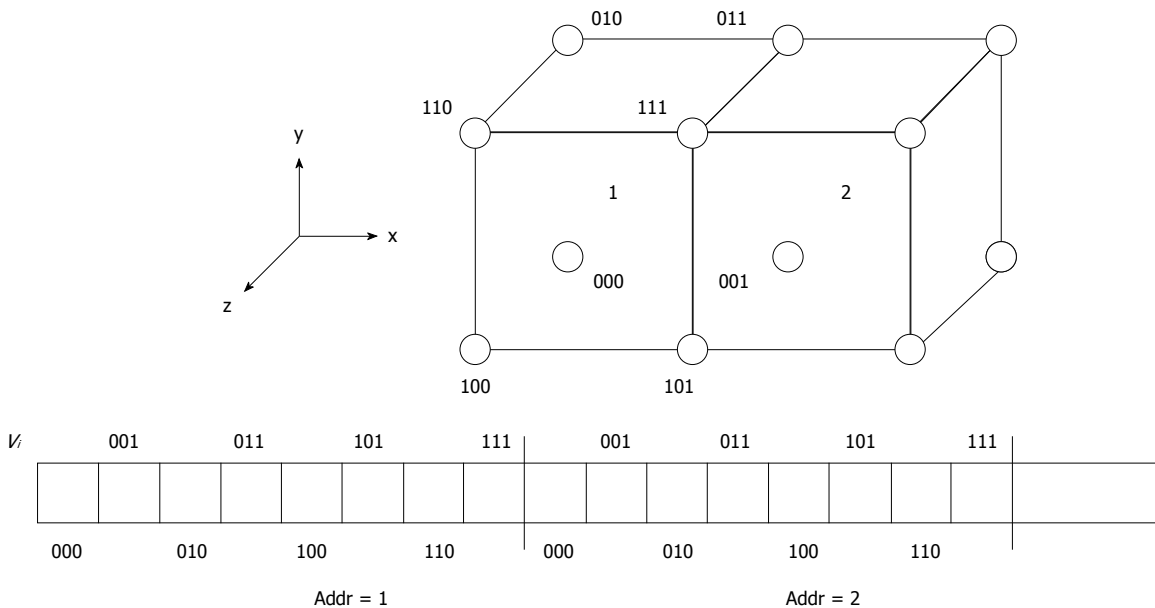


Figure 3 Cubic memory organization: Voxels are arranged in memory as cubes.

Accumulative rendering mode

We introduce the accumulated rendering mode in this system. Rather than revisiting the whole dataset when a new slice is updated, the previous rendering output is directly combined with the new slice instead. Through this computation, load is limited to only two slices, regardless of the size of the dataset. Modifications to the existing compositing methods will be required, and we would anticipate further refinement and utilize it to our advantage. We perform compositing for accumulative rendering using the following formula.

To accommodate the accumulative rendering mode, we use four framebuffers to store intermediate slices. This novel design is illustrated in Figure 4. We use four SRAM blocks as the framebuffers, two of which facilitate compositing and the remaining two as display buffers. This is used to overcome the problem of simultaneous read/write accesses, prohibited by the use of a single data bus.

During operation, the first slice only involves memory writing, where one SRAM from each framebuffer is accessed to store the acquired slice. In all other stages, the SRAM blocks interchange between memory reading and memory writing to ensure continuous flow, providing simultaneous reading and writing of rendering results. This is significant in the case of parallel pipelined coding, where memory read and write operations are continuous at each cycle, while the operations are only repeated once for each pixel. In single data placement systems, the read and write operation has to be time-multiplexed, resulting in longer time required for processing.

Optimization limitations

The introduction of these optimization techniques speeds up the rendering computation, but at the expense of several limitations. In online mode, a constant viewing configuration is employed. Viewing angles and distances

cannot be adjusted in this mode, as pre-computation of ray parameters assumes that the rays are always fixed in such a manner. This limitation is further reinforced with the method of combined slices, as a view change will require the whole dataset to be re-traversed instead of only visiting the existing rendering and the new slice.

Rendering is also performed only for parallel projections, which assume that all casted rays have the same direction. Further extensions can be done to include perspective projection ray casting through modification of the system and additional memory requirements to store different ray parameters for each pixel.

Also, cubic memory scheme organizes memory cubes continuously instead of interleaved. This introduces duplications of the voxels in memory, thus increasing the memory requirements to approximately eight times dataset size. However, the capacities supported by modern hardware and our system of 256 Mbytes on-board memory can easily satisfy these requirements.

Accumulative rendering mode is currently supported only for orthographic projection rendering. The viewing direction is always assumed to be perpendicular to the slices for accumulative rendering. Further refinement of this design can enable views from arbitrary directions. As this technique only renders two slices, cubic memory is not employed for rendering under this mode, but is used for rendering under arbitrary view configurations.

EXPERIMENTAL RESULTS AND DISCUSSION

The prototype system has been built and deployed with our collaborators at the National Cancer Center of Singapore (NCCS) for clinical experiments. A photo of the system is shown in Figure 5. This system includes the Optiscan FIVE1 LSCEM imaging device, the Celoxica

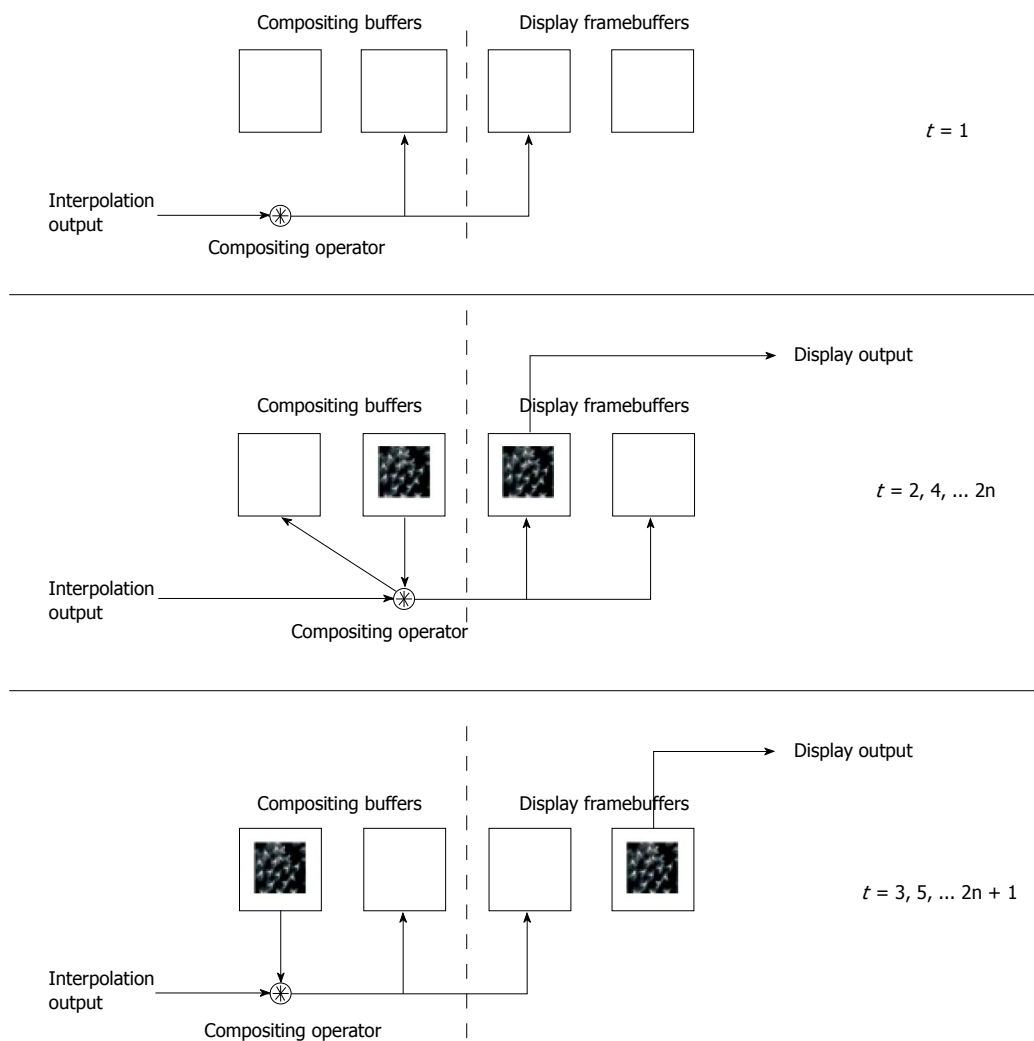


Figure 4 Framebuffers for accumulative rendering mode.

RC340 FPGA Development board, the relay switchbox hardware, and user interactivity tools.

We show the realtime online rendering results for a mouse tongue dataset in Figure 6. The rendering results are live results obtained during the imaging experiment. For rendering performance, the rendering system has to at least be able to perform faster than the rate slices are acquired in order to be meaningful. This rate is approximately 1.4 s per slice. The maximum number of slices is dependent on the significance of signal degradation as the focal plane advances deeper into the tissue. For our case, the maximal is around 40 slices.

The rendering results in Figure 6 show two different views. The orthographic projection renders the dataset by setting the viewing plane parallel to the acquired slices, under accumulative rendering mode. This shows perceived results viewed through consecutive depths. At the bottom right corner is a parallel projection with a specific viewing configuration, which shows an overview of the current dataset. Observations can be made through these different views across increasing thicknesses to the dataset.

The rendering will provide immediate perception of the acquired datasets at high quality. This is aimed towards

improving the imaging procedure and further enhancing the features and capabilities of LSCEM imaging. With this current platform, further extensions can be included, such as image processing techniques to provide automated diagnosis of cancer stages^[17].

The entire imaging procedure is now simplified, and can be fully operated by a single user. The user can adjust the probe either by a handheld device or through a fixed stand. Capture controls are fully automated, where the user is only required to initiate and terminate imaging controls. This enhances the imaging time as well as requiring less attention from the user to operate different controls at the same time.

CONCLUSION

We have presented our preliminary system to perform online rendering side-by-side with LSCEM imaging. By having an immediate knowledge of the dataset quality as well as the biological tissue conditions, alterations can be made on the spot. This will introduce the opportunity to change imaging conditions or medical decisions according to the online rendering results. This work is also mo-

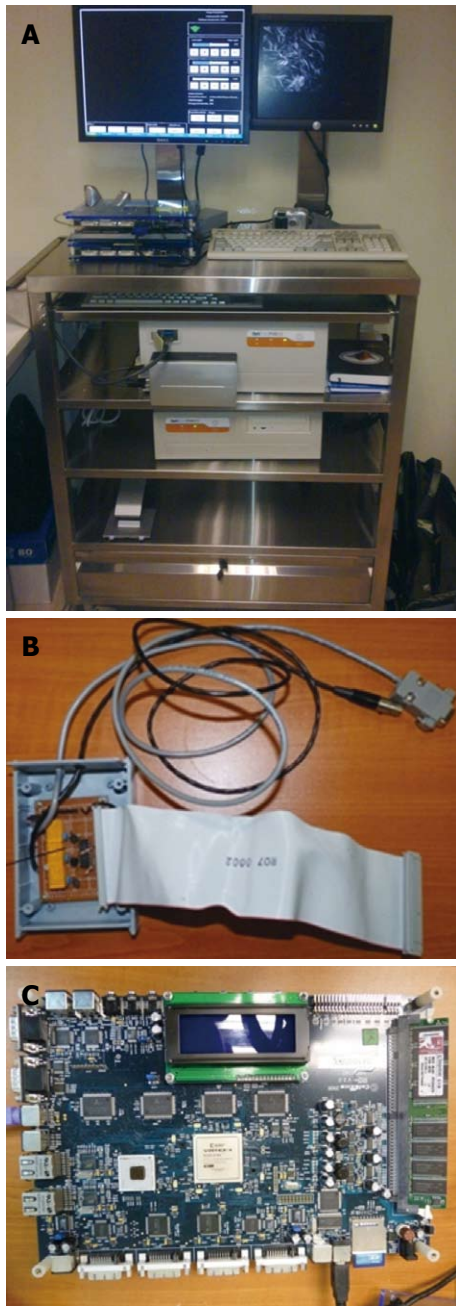


Figure 5 The Laser scanning confocal endomicroscope imaging-rendering prototype system.

tivated by the need to realize the quality of the captured datasets in realtime to reduce excessive time required for offline rendering.

The LSCEM procedure is also simplified and only one user is required to fully operate the system. Using electronic automation to substitute the footswitch as manual controls, the user is not required to repetitively control the imaging sequences to capture a full volumetric dataset. This reduces the time and attention required to perform LSCEM imaging.

We have also shown the FPGA as a viable solution for designing a system which can run the required tasks in parallel. Providing automated controls to substitute the

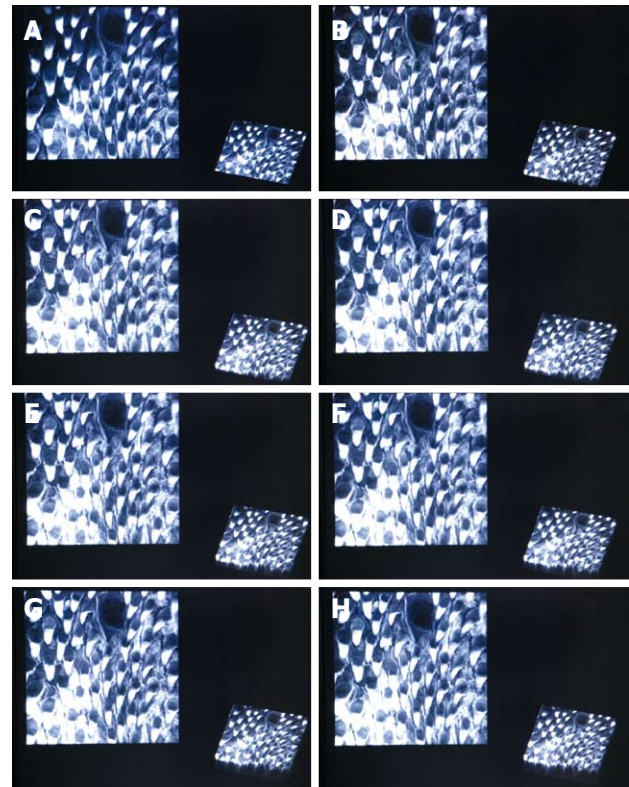


Figure 6 Online rendering of the mouse tongue surface across increasing number of slices. A: 2 slices; B: 10 slices; C: 15 slices; D: 20 slices; E: 25 slices; F: 30 slices; G: 35 slices; H: 38 slices.

prevailing manual capture, we make use of our custom built hardware to interface with the imaging system. Also the FPGA is able to provide synchronized controls between imaging and rendering, which is crucial in ensuring a stable operation. The full flexibility offered by FPGAs is important, considering future developments for embedded rendering systems to co-exist with imaging devices.

We would extend this work further by incorporating more sophisticated rendering procedures such as perspective projection rendering and interactive view changes in realtime.

ACKNOWLEDGMENTS

We are grateful to our clinic partners, Professor Soo Khee Chee, Professor Malini Olivo and Dr. Patricia SP Thong of National Cancer Centre Singapore.

REFERENCES

- 1 **Kak AC**, Slaney M. Principles of computerized tomographic imaging. IEEE Press, 1988
- 2 **Fenster A**, Downey BD. 3-D Ultrasound Imaging : A Review. New York, NY, ETATS-UNIS: Institute of Electrical and Electronics Engineers, 1996
- 3 **Elster AD**. Magnetic resonance imaging, a reference guide and atlas, 1986
- 4 **Thong PS**, Olivo M, Kho KW, Zheng W, Mancner K, Harris M, Soo KC. Laser confocal endomicroscopy as a novel technique for fluorescence diagnostic imaging of the oral cavity.

- J Biomed Opt* 2007; **12**: 014007
- 5 **Amos WB**, White JG. How the confocal laser scanning microscope entered biological research. *Biol Cell* 2003; **95**: 335-342
 - 6 **Laser Scanning Confocal Microscopy**. Last visited on July, 2010. Available from: URL: <http://www.olympusconfocal.com/theory/LSCMIntro.pdf>
 - 7 **Sandison DR**, Webb WW. Background rejection and signal-to-noise optimization in confocal and alternative fluorescence microscopes. *Appl Opt* 1994; **33**: 603-615
 - 8 **Gratton E**, Ven MJv. Laser Sources for Confocal Microscopy. In: Pawley JB, editor. Handbook of Biological Confocal Microscopy. New York: Plenum Press, 1995: 69-98
 - 9 **Tang M**, Wang H-N. Interactive Visualization Technique for Confocal Microscopy Images. In: Complex Medical Engineering, 2007. CME 2007. IEEE/ICME International Conference on 2007, 2007: 556-561
 - 10 **Ronneberger O**, Burkhardt H, Schultz E. General-purpose object recognition in 3D volume data sets using gray-scale invariants - classification of airborne pollen-grains recorded with a confocal laser scanning microscope. In: Pattern Recognition, 2002 Proceedings 16th International Conference on 2002, **2**: 290-295
 - 11 **Poddar AH**, Krol A, Beaumont J, Price RL, Slamani MA, Fawcett J, Subramanian A, Coman IL, Lipson ED, Feiglin DH, Dept of Electr, Computer Sci, Syracuse Univ, NY. Ultrahigh resolution 3D model of murine heart from micro-CT and serial confocal laser scanning microscopy images. In: Nuclear Science Symposium Conference Record, 2005 IEEE, 2005: 2615-2617
 - 12 **Pankajakshan P**, Bo Z, Blanc-Feraud L, Kam Z, Olivo-Marin JC, Zerubia J. Blind deconvolution for diffraction-limited fluorescence microscopy. In: 5th IEEE International Symposium on Biomedical Imaging: From Nano to Macro 2008, 740-743
 - 13 **Dey N**, Blanc-Feraud L, Zimmer C, Kam Z, Olivo-Marin JC, Zerubia J. A deconvolution method for confocal microscopy with total variation regularization. In: Biomedical Imaging: Nano to Macro, 2004 IEEE International Symposium on 2004, **2**: 1223-1226
 - 14 **Pankajakshan P**, Zhang B, Blanc-Feraud L, Kam Z, Olivo-Marin JC, Zerubia J. Parametric blind deconvolution for confocal laser scanning microscopy. *Conf Proc IEEE Eng Med Biol Soc* 2007; **2007**: 6532-6535
 - 15 **Lee HK**, Uddin MS, Sankaran S, Hariharan S, Ahmed S. A field theoretical restoration method for images degraded by non-uniform light attenuation : an application for light microscopy. *Opt Express* 2009; **17**: 11294-11308
 - 16 **Sang-Chul L**, Bajcsy P. Three-Dimensional Volume Reconstruction Based on Trajectory Fusion from Confocal Laser Scanning Microscope Images. In: Computer Vision and Pattern Recognition, 2006 IEEE Computer Society Conference on 2006, 2221-8222
 - 17 **Cheong L**, Lin F, Seah H. Embedded Computing for Fluorescence Confocal Endomicroscopy Imaging. *Journal of Signal Processing Systems* 2009; **55**: 217-228
 - 18 **Sakas G**, Vicker MG, Plath PJ. Case study: visualization of laser confocal microscopy datasets. Visualization '96 Proceedings, 1996: 375-379
 - 19 **Levoy M**. Display of surfaces from volume data. Computer Graphics and Applications, IEEE 1988, **8**: 29-37
 - 20 **Sakas G**, Grimm M, Savopoulos A. Optimized Maximum Intensity Projection (MIP), 1995
 - 21 **De Leeuw WC**, Van Liere R, Verschure PJ, Visser AE, Manders EMM, Van Drielf R. Visualization of time dependent confocal microscopy data. *Visualization 2000 Proceedings* 2000, 473-476, 593
 - 22 **Kajiya JT**. The rendering equation. *SIGGRAPH Comput Graph* 1986; **20**: 143-150
 - 23 **Nelson M**. Optical Models for Direct Volume Rendering. IEEE Transactions on Visualization and Computer Graphics 1995, **1**: 99-108
 - 24 **Kajiya JT**. Ray tracing parametric patches. In: Proceedings of the 9th annual conference on Computer graphics and interactive techniques. Boston, Massachusetts, United States: ACM, 1982: 245-254
 - 25 **Kajiya JT**. New techniques for ray tracing procedurally defined objects. *SIGGRAPH Comput Graph* 1983; **17**: 91-102
 - 26 **Kajiya JT**, Herzen BPV. Ray Tracing Volume Densities. *ACM SIGGRAPH Computer Graphics* 1984; **18**: 165-174
 - 27 **Fishman EK**, Magid D, Robertson DD, Brooker AF, Weiss P, Siegelman SS. Metallic hip implants: CT with multiplanar reconstruction. *Radiology* 1986; **160**: 675-681
 - 28 **Avila RS**, Sobierajski LM, Kaufman AE. Towards a comprehensive volume visualization system. In: Proceedings of the 3rd conference on Visualization '92. Boston, Massachusetts: IEEE Computer Society Press, 1992: 13-20
 - 29 **Avila R**, He T, Hong L, et al. VolVis: a diversified volume visualization system. In: Proceedings of the conference on Visualization '94. Washinton, D.C.: IEEE Computer Society Press, 1994: 31-38
 - 30 **Sobierajski LM**, Kaufman AE. Volumetric Ray Tracing. Proceedings of the 1994 symposium on Volume visualization 1994, **1**: 11-18
 - 31 **Kniss J**, Kindlmann G, Hansen C. Multidimensional Transfer Functions for Interactive Volume Rendering. IEEE Transactions on Visualization and Computer Graphics 2002, **8**
 - 32 **Wolf I**, Vetter M, Wegner I, Böttger T, Nolden M, Schöbinger M, Hastenteufel M, Kunert T, Meinzer HP. The medical imaging interaction toolkit. *Med Image Anal* 2005; **9**: 594-604
 - 33 **Tian J**, Xue J, Dai Y, Chen J, Zheng J. A novel software platform for medical image processing and analyzing. *IEEE Trans Inf Technol Biomed* 2008; **12**: 800-812
 - 34 **Tandjung SS**, Zhao F, Lin F, Qian K, Seah HS. Synchronized Volumetric Cell Image Acquisition with FPGA-Controlled Endomicroscope. In: Proceedings of the 2009 International Conference on Embedded Systems & Applications, ESA; 2009 July 13-16, 2009; Las Vegas Nevada, USA; 2009

S- Editor Cheng JX L- Editor O'Neill M E- Editor Ma WH

Automation of immunohistochemical evaluation in breast cancer using image analysis

Keerthana Prasad, Avani Tiwari, Sandhya Ilanthodi, Gopalakrishna Prabhu, Muktha Pai

Keerthana Prasad, Manipal Centre for Information Science, Manipal University, Manipal 576104, Karnataka, India
Avani Tiwari, Muktha Pai, Department of Pathology, Kasturba Medical College, Manipal University, Manipal 576104, Karnataka, India

Sandhya Ilanthodi, Department of Pathology, A.J Institute of Medical Sciences, Manipal 576104, Karnataka, India
Gopalakrishna Prabhu, Department of Biomedical Engineering, Manipal Institute of Technology, Manipal 576104, Karnataka, India

Author contributions: Prasad K designed and carried out this research; Tiwari A carried out the sample collection, tissue processing and acquisition of images; Tiwari A, Pai M and Ilanthodi S provided the readings for the manual evaluations; Prabhu G supervised this research; all authors contributed to the writing of this paper.

Correspondence to: Keerthana Prasad, Assistant Professor, Manipal Centre for Information Science, LG02, Academic Block 5, M.I.T Campus, Manipal 576104, Karnataka, India. keerthana.prasad@manipal.edu

Telephone: +91-984-5308499 Fax: +91-820-2925033

Received: March 18, 2010 Revised: March 31, 2011

Accepted: April 7, 2011

Published online: April 10, 2011

developed software (TissueQuant). A comparison of the results from image analysis and manual scoring of ER, PR and HER-2/neu was also carried out.

RESULTS: The performance of the automated analysis in the case of ER, PR and HER-2/neu expressions was compared with the manual evaluations. The performance of the automated system was found to correlate well with the manual evaluations. The inter-observer variations were measured using Spearman correlation coefficient r and 95% confidence interval. In the case of ER expression, Spearman correlation $r = 0.53$, in the case of PR expression, $r = 0.63$, and in the case of HER-2/neu expression, $r = 0.68$. Similarly, intra-observer variations were also measured. In the case of ER, PR and HER-2/neu expressions, $r = 0.46, 0.66$ and 0.70 , respectively.

CONCLUSION: The automation of breast cancer diagnosis from immunohistochemically stained specimens is very useful for providing objective and repeatable evaluations.

© 2011 Baishideng. All rights reserved.

Abstract

AIM: To automate breast cancer diagnosis and to study the inter-observer and intra-observer variations in the manual evaluations.

METHODS: Breast tissue specimens from sixty cases were stained separately for estrogen receptor (ER), progesterone receptor (PR) and human epidermal growth factor receptor-2 (HER-2/neu). All cases were assessed by manual grading as well as image analysis. The manual grading was performed by an experienced expert pathologist. To study inter-observer and intra-observer variations, we obtained readings from another pathologist as the second observer from a different laboratory who has a little less experience than the first observer. We also took a second reading from the second observer to study intra-observer variations. Image analysis was carried out using in-house

Key words: Automation; Breast cancer diagnosis; Computer aided diagnosis; Image analysis; Immunohistochemical study

Peer reviewer: Songsak Petmitr, PhD, Associate Professor, Department of Tropical Nutrition and Food Science, Mahidol University, 420/6 Ratchawithi Road, Bangkok 10400, Thailand

Prasad K, Tiwari A, Ilanthodi S, Prabhu G, Pai M. Automation of immunohistochemical evaluation in breast cancer using image analysis. *World J Clin Oncol* 2011; 2(4): 187-194 Available from: URL: <http://www.wjgnet.com/2218-4333/full/v2/i4/187.htm> DOI: <http://dx.doi.org/10.5306/wjco.v2.i4.187>

INTRODUCTION

Cancer of the breast is the second most common human

neoplasm and accounts for approximately one quarter of all cancers in females after cervical carcinoma^[1]. The accurate diagnosis of cancer plays a very important role in the treatment of patients with neoplastic breast disease. Immunohistochemical evaluation of hormone receptor expressions in tumor cell nuclei is an integral part of routine breast cancer diagnosis and provides important information for prognosis and choice of therapeutic approach.

Estrogen receptor (ER), progesterone receptor (PR) and human epidermal growth factor receptor-2 (HER-2/neu) over-expression as a predictor for herceptin therapy are crucially important in the biology of breast carcinoma. ER and PR expressions are the only predictive factors with proven usefulness in selecting patients who are likely to respond to adjuvant endocrine therapy. Patients lacking these receptors tend to have a shorter disease-free survival and earlier recurrence than those expressing these receptors^[2]. In around 20%-30% of breast carcinoma, HER-2/neu is amplified and over-expressed. It is associated with an adverse prognosis independent of other prognostic factors in most cases and appears to be stronger in node-positive carcinoma. Immunohistochemical reactivity of tumor cells to ER, PR, and HER-2/neu helps the clinician to establish the mode of therapy and indicates the survival and recurrence rates of the tumor. The recurrent tumor or metastatic tumor may not show the same immunoreactivity, and the unstable status of HER-2/neu in breast cancer is clinically significant^[3]. Receptor status in recurrent or metastasized breast cancer can be different from the original tumor. It was reported that ER status changed in around 33% of cases, and HER-2/neu status changed in around 10%.

In addition, ER-positive and ER-negative breast cancers have distinct disease-specific patterns^[4]. A molecular classification of breast cancer is also performed based on their reactivity. The treatment protocol varies with the pattern of reactivity and is based on the molecular classification. Immunohistochemistry (IHC) is expected to play an increasingly important role in the clinical management of breast cancer^[5].

The main challenges that pathologists are currently facing are productivity, accuracy and objective evaluation. Manual evaluation takes more time and resources. It is less accurate and is also highly subjective. Qualitatively, the immunohistochemically stained specimen can be evaluated visually as the presence of a specific color. However, to perform a quantitative evaluation, the number of stained cell nuclei and/or the amount of specimen that has been stained needs to be measured. For this purpose, computerized image analysis based methods are needed.

Traditionally, pathologists distinguish between positive and negative results based on visual judgment of the percentage of positive tumor cells, the cutoff being arbitrarily defined between 5% and 45%^[6-9]. Some studies report the use of semiquantitative scores to assess nuclear staining intensity as a marker of the number of receptors per cell^[10-13]. Diverse computerized image analysis systems have also been employed to provide more standardized data for quantification and were found to correlate well

with semiquantitative scoring methods^[14-16]. A large number of studies have reported the use of image analysis as a means of evaluating histological staining. Substantial efforts have been made to correlate the evaluations made by experienced pathologists with quantitative values^[17-26]. Initial studies on the use of computerized image analysis were limited to evaluation of images based on gray levels^[27,28]. Recently, studies have used the color spectrum of histological stains rather than gray levels for analysis of the images to discriminate cellular details^[29,30]. The receptors can be accurately quantified by measuring the strength of expression^[13]. Hence, automation of quantification could be very useful for the evaluation of histological staining for the diagnosis of breast cancer. However, their use in the routine diagnostic laboratory is limited due to the high cost and the complexity of the image analysis systems^[17].

The goals of the present study were to establish the validity of the in-house developed image analysis system (TissueQuant version 1.0) for classification of the images for the diagnosis of breast cancer and to determine data variability due to investigator bias by calculating inter- and intra-observer variability in the case of manual evaluations. Each case was subjected to immunohistochemical evaluation along with the image analysis system and validation was performed by comparing visual and computer analysis of the same tissue fields.

MATERIALS AND METHODS

Specimens from sixty patients were subjected to immunohistochemistry separately with antibodies for ER, PR and HER-2/neu. The patient's name, age, sex and clinical data were recorded. Out of a total of 60 cases studied 23 (38%) were younger than 50 years while the remaining 37 (62%) were older than 50 years of age. The youngest patient was 30 years and the oldest was 72 years old. The mean age of the patients was 52.5.

The specimens were received in 10% formalin and were sampled after fixation for less than 24 h. Care was taken not to over fix the tissue, as this would interfere with the receptor analysis. The specimens were examined grossly for ulceration, peau d' orange, and retraction of nipple. The deeper resected margin was stained with India ink. Adequate numbers of sections were taken from the nipple and areola, the tumor proper, all the margins with and without tumor, adjacent breast parenchyma and other relevant areas.

Staining protocol

Hematoxylin and eosin (HE) was used as a routine stain to establish the histopathological diagnosis and for general study of the tissue; the markers ER, PR and Her-2/neu were assessed using immunohistochemistry; image analysis was performed using TissueQuant software for each immunohistochemically stained slide.

Immunohistochemistry staining for ER, PR and HER-2/neu was carried out by the polymer labeling 2-step method using the Super Sensitive™ Polymer- HRP IHC detection system (Biogenex).

Slide preparation

Slides were washed in soapy water and then washed three times with distilled water. Thereafter, they were rinsed in methanol and dried at room temperature. Poly-L-lysine solution was applied to the slides which were dried overnight at room temperature. Sections were treated as follows: (1) 5 μ thick sections were cut and mounted on the slides coated with poly-L-lysine. The sections were deparaffinized with 3 changes in xylene, 2 changes in methanol and then a decreasing concentration of isopropyl alcohol (i.e. 90%, 70%, 50% alcohol) and finally in distilled water for 5 min each; (2) The slides were then immersed in 3% hydrogen peroxide for 20 min to quench the endogenous peroxidase; (3) Antigen retrieval and unmasking was carried out by immersion in citrate buffer and incubation in a pressure cooker with 250 mL of water at 100°C for 15-20 min; (4) After cooling at room temperature, the slides were washed in buffer (0.1 mol/L Tris-HCl, 0.15 mol/L NaCl, pH 7.5) with the washing procedure carried out in a jar containing Tris buffer and immersing the slides for two 5 min periods (total of 10 min); (5) This was followed by incubation for 20 min in the Power block (buffered casein solution with sodium azide) to suppress non-specific binding of subsequent reagent; (6) The slides were then incubated in mouse primary antibody for 75 min at room temperature, after which they were washed in Tris buffer. For the ER study, mouse monoclonal antibody diluted with HK941-YAK in buffered glycine phosphate pH 7.1, 6% protein and 0.09% sodium azide was used. For the PR study, mouse monoclonal antibody in phosphate buffered saline pH 7.6 containing 1% bovine serum albumin (BSA) was used. For the HER-2/neu study, mouse monoclonal antibody from tissue culture supernatant diluted in phosphate buffered saline pH 7.6 containing 1% BSA and 0.09% sodium azide was used; (7) The slides were then immersed in Super Enhancer for 30 min, after which the washing procedure was repeated; (8) The slides were immersed again in Poly HRP (horseradish peroxidase) for 20 min, after which they were washed with Tris buffer followed by distilled water for 5 min each; (9) The slides were then treated with diaminobenzidine (DAB) chromogen for 5 min to develop the brown color; (10) Thorough washing in Tris buffer and distilled water was then performed; and (11) Counter staining with Meyer's hematoxylin was performed for 1 min and then the slides were washed in tap water. The slides were dried and mounted with a cover slip and mounting media.

Immunohistochemistry scoring

ER and PR expressions: According to the International Breast Cancer Study Group, ER and PR were graded as: (1) None (grade 0): none of the tumor cells showed nuclear staining; (2) Low (grade 1): 1%-9% of cells showed nuclear positivity; and (3) High (grade 2): $\geq 10\%$ of the cells showed nuclear positivity.

When considering the hormone receptor status, grade 1 and 0 were considered hormone receptor negative, and grade 2 was considered positive.

HER-2/neu expression: According to US FDA panel findings, (1) Grade 3: cell surface protein expression-positive: defined as uniform intense membrane staining of $> 30\%$ of invasive tumor cells; (2) Grade 2: cell surface protein expression- equivocal: defined as complete membrane staining that is either non uniform or weak in intensity but with obvious circumferential distribution in at least 10% of cells; and (3) Grade 0 or 1: cell surface protein expression- negative: no staining or weak, incomplete membrane staining in any proportion of the tumor cells.

When considering the HER-2/neu membrane status, grade 0, 1 and 2 were considered negative and grade 3 was considered positive.

Image analysis

Images were analyzed using the in-house developed software (TissueQuant). The facility for choosing the color representing the maximum density of hormone expression as a reference color is provided in the software. Using this facility, the color setting was used for analysis purposes. The software assigns scores to the various shades of the color represented by each pixel of the image, based on how close the shade is to the reference color. Using these values, the total hormone expression in the image is quantified. For this, the image is represented in the HSI color model. Gaussian weighting functions are used for scoring the shades. The widths of the Gaussian weighting functions are decided by the different ranges for the hue, saturation and intensity components. These values decide the range of shades of the color which should be considered as positive staining. These weighting functions provide the flexibility of fine adjustments of the color shades to be included.

Considering two parameters based on the color scores, a classification system was developed to classify a particular case as positive, negative and strongly positive. There were two parameters assigned-Mean and Mean-Max. Mean was the main criterion on which the decision was made. It represents the average hormone expression present in the image. Mean-Max was used as a helpful parameter for decision-making. This represents the maximum depth of the color shade present in the image. This was useful when the expression was concentrated in a small area. A grade was calculated based on the above two scores.

A screenshot of the software is shown in Figure 1. The user is provided with a facility to open the image and click on the region of the image with the reference pixel color. A set of sliders are provided to adjust the color parameters on the lower mid panel. The centers and widths of the Gaussian weighting functions can be adjusted with these sliders. The color parameters are set this way to calculate the color score for each pixel which is mapped from 0 to 255 for the purpose of display as a grayscale image in the right upper panel of the user interface. The color score and the color settings for the particular study are displayed just below the resulting image. This facilitates user interaction to select the appropriate color settings for the quantification. A "Save" button is also provided which

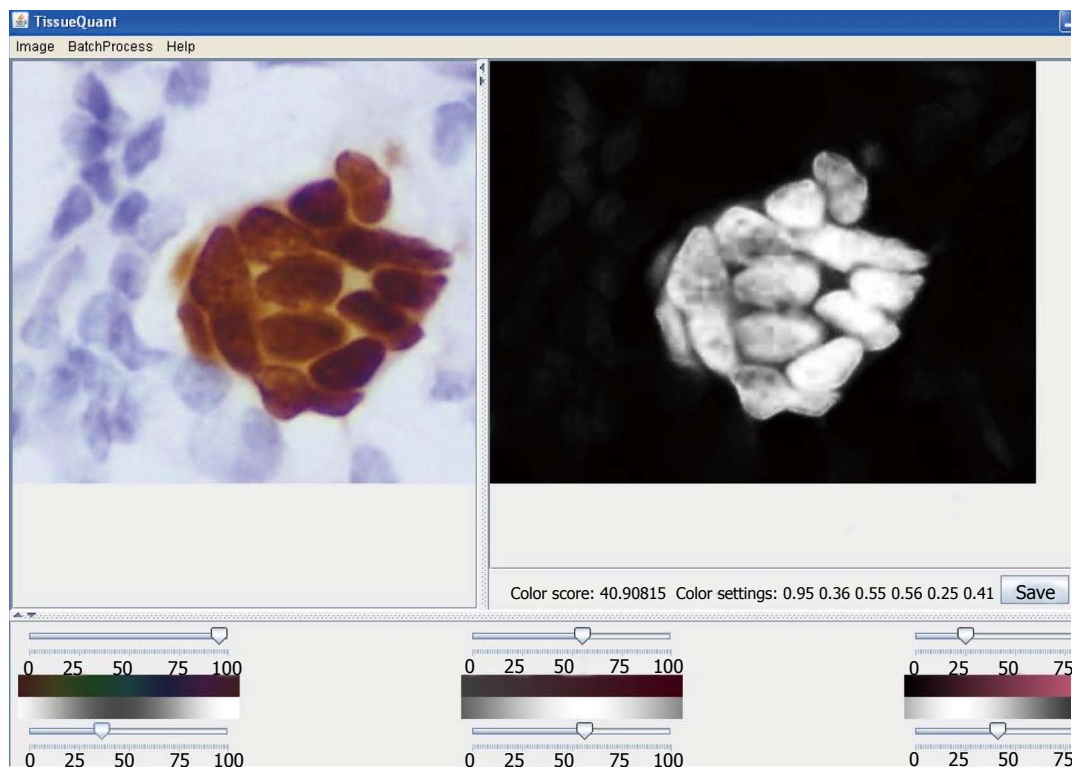


Figure 1 Screenshot of the TissueQuant software. On the left panel of the main window the original image is opened. The right panel displays the color score representation of the image. In the lower panel are the sliders which could be adjusted to select the color shade of interest.

facilitates saving of the resulting image. We could also save the color settings by specifying a name for the particular study. These color settings can be used for batch processing of image sets with the same color settings in an automated manner. To work on huge sets of images with the same color setting directly, the “Batch Analysis” option is used. The directory in which the images are saved, the color setting and the image type used for the batch analysis need to be specified by the user. All images in the specified directory are processed and the resulting images are stored in the ‘result-images’ directory, which is generated under the specified directory. The mean color score and the image name are stored in an MS Excel file in the same directory.

Manual method and image analysis

The specimens from all sixty cases were stained separately for ER, PR and HER-2/neu. All cases were assessed by manual grading as well as image analysis. The manual grading was carried out by an experienced expert pathologist. To study inter-observer and intra-observer variations, we obtained readings from another pathologist as the second observer from a different laboratory who has a little less experience than the first observer. We also took a second reading from the second observer after 30 d to study intra-observer variations.

For statistical analysis of the results, we used SPSS 11.5 for Windows and GraphPad Prism 4.03. The inter-observer and intra-observer variations were evaluated with SPSS software. The Spearman correlation coefficient was obtained using GraphPad Prism software. A ROC

curve was drawn using Microsoft Excel software using the sensitivity and specificity of the algorithm for each of the expressions.

RESULTS

A comparison of the grading of the cases by the expert and the image analysis software TissueQuant for ER, PR and HER-2/neu expressions are shown in Tables 1-5 and Figure 2.

ER

All cases were assessed by manual grading as well as image analysis. Thirty cases with grade 0 on manual grading showed a similar grade on image analysis. Out of 12 cases with a manual grading of 0, 6 showed grade 1 and 6 showed grade 2 on image analysis. Two cases with manual grade 1 showed grade 2 on image analysis. All cases with manual grade 2 showed a similar grade on image analysis. These findings were statistically highly significant (Table 1).

The ER expression evaluation performed by the expert was compared with the evaluation by the second pathologist. Evaluation by both pathologists in 24 cases of grade 0 out of 42 cases, 2 cases of grade 1 out of 4 cases and 8 cases of grade 2 out of 14 cases matched correctly. The ER expression evaluation was repeated by the second pathologist and was compared to the first evaluation. The evaluation in both readings matched in 19 cases of grade 0 out of 26 cases, 12 cases of grade 1 out of 21 cases and 6 cases of grade 2 out of 13 cases.

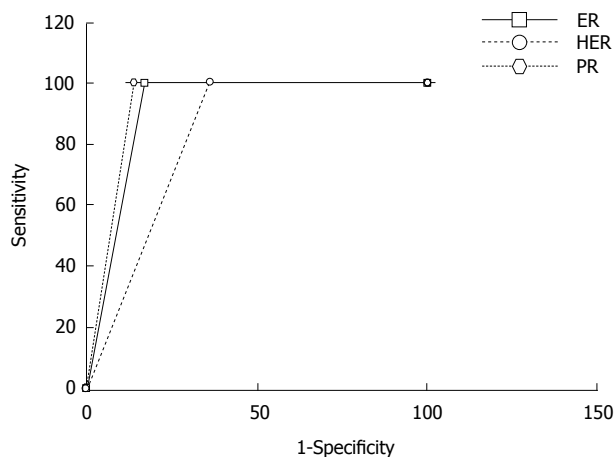


Figure 2 ROC curves for the automated evaluation of estrogen receptor, progesterone receptor and human epidermal growth factor receptor-2 expression images using TissueQuant. For all three expressions the sensitivity of 100% is maintained, the specificity for PR expression is best at, 86%, for ER the specificity is 82.3% and for HER-2/neu expression the specificity is least at, 64.3%. ER: Estrogen receptor; PR: Progesterone receptor; HER-2/neu: Human epidermal growth factor receptor-2.

Table 1 Comparison of manual grading and image analysis of estrogen receptor

Manual grading	Image analysis			Total
	Grade 0	Grade 1	Grade 2	
Grade 0	30	6	6	42
Grade 1	0	2	2	4
Grade 2	0	0	14	14
Total	30	8	22	60

PR

PR status was also assessed by manual grading as well as image analysis. Thirty five cases with grade 0 on manual grading showed a similar grade on image analysis. Out of 8 cases with a manual grading of 0, 6 showed grade 1 and 2 showed grade 2 on image analysis. Five cases with manual grade 1 showed grade 2 on image analysis. All cases with manual grade 2 showed a similar grade on image analysis. These findings were statistically highly significant (Table 2).

The PR expression evaluation performed by the expert was compared with the evaluation by the second pathologist. Evaluation by both pathologists in 32 cases of grade 0 out of 43 cases, 6 cases of grade 1 out of 7 cases and 6 cases of grade 2 out of 10 cases matched correctly.

The PR expression evaluation was repeated by the second pathologist and was compared to the first evaluation. The evaluation in both readings matched in 28 cases of grade 0 out of 34 cases, 8 cases of grade 1 out of 18 cases and 3 cases of grade 2 out of 8 cases.

HER-2/neu

For HER-2/neu status, 6 cases with manual grade 0 showed a similar grade on image analysis. One case with a manual grade of 0 showed grade 2 on image analysis. None of the cases showed grade 1 on manual as well as

Table 2 Comparison of manual grading and image analysis of progesterone receptor

Manual grading	Image analysis			Total
	Grade 0	Grade 1	Grade 2	
Grade 0	35	6	2	43
Grade 1	0	2	5	7
Grade 2	0	0	10	10
Total	35	8	17	60

Table 3 Comparison of manual grading and image analysis of human epidermal growth factor receptor-2

Manual grading	Image analysis				Total
	Grade 0	Grade 1	Grade 2	Grade 3	
Grade 0	6	0	1	0	7
Grade 1	0	0	0	0	0
Grade 2	0	0	2	5	7
Grade 3	0	0	0	46	46
Total	6	0	3	51	60

image analysis. Five cases with manual grade 2 showed grade 3 on image analysis. All 46 cases with manual grade 3 showed a similar grade on image analysis. These findings were highly significant (Table 3).

HER-2/neu expression evaluation performed by the expert was compared with the evaluation by the second pathologist. Evaluation by both pathologists in 6 cases of grade 0 out of 7 cases, 3 cases of grade 2 out of 7 cases and 29 cases of grade 3 out of 46 cases matched correctly.

HER-2/neu expression evaluation was repeated by the second pathologist and was compared to the first evaluation. The evaluation in both readings matched in 6 cases of grade 0 out of 7 cases, 2 cases of grade 2 out of 7 cases and in all 46 cases of grade 3.

DISCUSSION

Various types of solutions are available to quantify staining intensity and range from inexpensive, general purpose software to specific, expensive software. Some of the image analysis systems used for such studies are SAMBA, Image Pro Plus, Metaview, Lucia software, and BioQuant Nova Prime. Charpin *et al* used Metaview software for staining intensity quantification. This is a general purpose image processing software^[31]. Suitable threshold values for the Red (R), Green (G) and Blue (B) components are selected to choose the stained area. The amount of positively stained area gives the measure of staining. Charpin *et al*^[32] used the SAMBA 4000 image analysis system for quantification of hormone receptor expression. For each marker's positive cell surface, integrated and mean optical densities and IOD histograms were compared. Pauschinget *et al*^[33] and Soukupova *et al*^[34] made use of Lucia software for stain quantification, which uses a measure of optical density. Diaz Encarnacion *et al*^[31] and Niendorf *et al*^[35] used a threshold and area measurement approach. Hatanaka *et al*^[20] used WinROOF with macroinstructions for analyzing each captured area. Lehr *et al*^[17] used Adobe

Table 4 Results of the classification of estrogen receptor, progesterone receptor and human epidermal growth factor receptor-2 expression images

	True positive	True negative	False positive	False negative	Sensitivity (%)	Specificity (%)	PPV ¹ (%)	NPV ² (%)
ER expression	14	38	8	0	100	82.6	63.6	100
PR expression	10	43	7	0	100	86.0	58.8	100
HER-2/neu expression	46	9	5	0	100	64.3	90.2	100

¹PPV: Positive predictive value; ²NPV: Negative predictive value. It can be seen that the sensitivity has been maintained at 100%. The specificity of the evaluations for ER and PR is good. The specificity of HER-2/neu expression is comparatively less than the ER and PR expression evaluations. ER: Estrogen receptor; PR: Progesterone receptor; HER-2/neu: Human epidermal growth factor receptor-2.

Table 5 Spearman correlation coefficient (95% confidence interval) of the different evaluations

	Expert vs automated analysis ¹	Expert vs pathologist ²	Pathologist reading 1 vs pathologist reading 2 ³
ER expression	0.73 (0.59 to 0.83)	0.53 (0.32 to 0.69)	0.46 (0.24 to 0.64)
PR expression	0.82 (0.73 to 0.90)	0.63 (0.45 to 0.76)	0.66 (0.49 to 0.78)
HER-2/neu expression	0.92 (0.88 to 0.96)	0.68 (0.52 to 0.80)	0.70 (0.54 to 0.81)

¹Represents the correlation of the automated analysis with the expert's evaluation; ²Represents the correlation between two pathologists; ³Represents the correlation between readings by the same pathologists taken at different time periods. It can be seen that the Spearman correlation coefficients for evaluations by automated analysis are better for all receptor expressions.

Photoshop-based image analysis to quantify hormone receptor expression in breast cancer. The feature selection was done with the Magic Wand tool which could reliably select all immunostained nuclei. The nuclear immunostaining index was calculated as the difference between nuclear and background immunostaining intensity. Vrekoussis *et al.*^{36]} reported the use of freeware ImageJ for the analysis of immunohistochemically stained sections of breast cancer. McCabe *et al.*^{37]} and Chung *et al.*^{38]} carried out quantitative analysis of hormone receptor expressions in breast cancer using the AQUA system. BioQuant Nova Prime is an advanced image analysis tool designed for biomedical research. Ariol SL 50 is an automated microscope slide analysis tool, which acquires monochrome images through three bright field filters, using cell masking templates and applies area analysis. Image Pro Plus (Media Cybernetics) and EMPIX Imaging solutions are also being used for stain quantification. Sharangpani *et al.*^{39]} developed a semi-automatic system to quantify estrogen and progesterone receptor immunoreactivity in human breast cancer. All these applications work on the basis of threshold and area measurement or change in optical density. It is not always possible to select appropriate R, G and B thresholds to suitably select shades of a particular color. Hence, the approach of threshold and area measurement is inadequate. In addition, when a tissue section is studied for a particular substance, other components present in the section may also take up the stain, expressing different colors. In such cases, the change in optical density is not a suitable indicator to measure the amount of the substance under study. However, the in-house developed software, TissueQuant, overcomes all these drawbacks by facilitating discrimination between colors and also between depths of color. Thus, it provides a fully automated solution for more efficient quantification of staining intensity.

Automation of image analysis holds promise for im-

proving inter- and intra-observer reproducibility which is the main problem with manual analysis. However, the lack of standards in system performance makes automation less reliable. Automation could also face problems with variations in illumination while imaging, variations in staining intensities, and section thickness. These could be solved with automated sectioning and staining systems. Standardized guidelines for transmission of baseline colors are very important since the evaluation is based on intensity. The clinical utility of automated analysis depends on strict adherence to quality assurance of the systems. Discrepancies in evaluation could be really serious; hence, automated evaluation does not eliminate the role of the pathologist. In our study, the focus was to identify all possible positive cases to ensure there were no false negative results. Once this is done, the expert pathologist can prioritize the slides to confirm the evaluation of the automated system.

The benefit of automation and computer-aided diagnosis has been demonstrated here. It was observed that there was a very good correlation between image analysis and expert opinion in evaluating the ER, PR and HER-2/neu expression images. The system was designed to avoid any false negative findings, hence, the specificity was compromised to obtain 100% sensitivity. This can be seen from the ROC curve in Figure 2. Table 5 shows the inter-observer variations and the intra-observer variations. It can be seen that the correlation between two readings by the same observer was slightly higher than the correlation of the readings by the two pathologists in the PR and HER-2/neu expression images. However, in the case of the ER expression images, intra-observer variation was greater than inter-observer variation. It was observed that in the majority of cases of mismatch, the grade 0 cases were mostly evaluated as grade 1 rather than grade 2, and similarly cases of grade 3 were mostly evaluated as grade 2 rather than grade 1. The automated analysis correlated best with the expert's opinion

in all three cases and this was significantly higher than the correlation between the two different observers and between two readings by the same observer.

This paper presents a technique for automation of the diagnosis of breast cancer from immunohistochemically stained biopsy specimens. Our goal was to provide 100% sensitivity and the software was successfully used to efficiently classify the cases. It was also demonstrated that the manual evaluation introduced a lot of variation, whereas the automated analysis provided an objective evaluation and was repeatable. Such automation could facilitate fast and efficient diagnosis of breast cancer and eliminate human errors, to a large extent. However, the results reported here could be further improved with the use of neural networks or other such classification models.

COMMENTS

Background

Cancer of the breast is the second most common human neoplasm and accounts for approximately one quarter of all cancers in females after cervical carcinoma. Immunohistochemical evaluation of hormone receptor expressions in tumor cell nuclei is an integral part of routine breast cancer diagnosis and provides important information for prognosis and choice of therapeutic approach. The main challenges that pathologists are currently facing are productivity, accuracy and objective evaluation. Pure visual estimates of immunohistochemically stained biopsy specimens provide very crude results with poor inter-observer and intra-observer reproducibility. For this purpose, computerized image analysis based methods are needed.

Research frontiers

Many studies have been carried out using computerized image analysis for the automation of evaluation. The use of various software packages such as ImageJ, the AQUA system, Image Pro Plus, and Adobe Photoshop has been reported. Another area which has seen very good advancement is the high throughput technology called tissue microarray (TMA) which generates a huge number of images in a fully automated and standardized manner which also makes it best suited for automation of evaluation.

Innovations and breakthroughs

In this article, the authors introduce the in-house developed software, TissueQuant, for automation of the evaluation of images of immunohistochemically stained biopsy specimens. The method they proposed provides a fully automated solution to these evaluations. The algorithm was designed to obtain 100% sensitivity. The inter-observer and intra-observer variations are reported. In addition, the correlation of the automated analysis with the expert's evaluation is also reported. It can be seen that the automated evaluation correlated well with the expert and overcame the problem of inter-observer and intra-observer variation.

Applications

The proposed method can be used to automate evaluations of images generated with the Tissue MicroArray technique so as to handle high throughput. The same technique can also be modified to evaluate any image where staining intensity needs to be assessed for decision-making.

Terminology

Estrogen receptor (ER), progesterone receptor (PR) and human epidermal growth factor receptor-2 (HER-2/neu) are specific hormone receptors which are expressed when stained with the respective immunohistochemical stains.

Peer review

Keerthana Prasad and colleagues demonstrated that the automation of breast cancer diagnosis from immunohistochemically stained specimen is a useful tool to provide objective and repeatable evaluations.

REFERENCES

- 1 Ellis IO, Shnitt SJ, Sastre-Garau X, Bussolati G, Tavassoli FA, Eusebi V. "Invasive Breast Carcinoma", In: Tavassoli FA, Devilee P, editors. Pathology and genetics- tumors of the breast and female genital organs World Health Organization classification of tumors. Lyon: IARC Press, 2006: 9-110
- 2 Almasri NM, Al Hamad M. Immunohistochemical evaluation of human epidermal growth factor receptor 2 and estrogen and progesterone receptors in breast carcinoma in Jordan. *Breast Cancer Res* 2005; **7**: R598-R604
- 3 Wilking U, Karlsson E, Skoog L, Hatschek T, Lidbrink E, Elmberger G, Johansson H, Lindström L, Bergh J. HER2 status in a population-derived breast cancer cohort: discordances during tumor progression. *Breast Cancer Res Treat* 2010; Jul 14
- 4 Osborne JR, Port E, Gonen M, Doane A, Yeung H, Gerald W, Cook JB, Larson S, "18F-FDG PET of locally invasive breast cancer and association of estrogen receptor status with standardized uptake value: microarray and immunohistochemical analysis". *J Nucl Med* 2010; **51**: 543-550
- 5 Brennan DJ, Gallagher WM. Prognostic ability of a panel of immunohistochemistry markers - retailoring of an 'old solution'. *Breast Cancer Res* 2008; **10**: 102
- 6 Raymond WA, Leong AS. Oestrogen receptor staining of paraffin-embedded breast carcinomas following short fixation in formalin: a comparison with cytosolic and frozen section receptor analyses. *J Pathol* 1990; **160**: 295-303
- 7 Molino A, Micciolo R, Turazza M, Bonetti F, Piubello Q, Corgnati A, Sperotto L, Martignoni G, Bonetti A, Nortilli R. Estrogen receptors in 699 primary breast cancers: a comparison of immunohistochemical and biochemical methods. *Breast Cancer Res Treat* 1995; **34**: 221-228
- 8 Veronese SM, Barbareschi M, Morelli L, Aldovini D, Mauri FA, Caffo O, Gambacorta M, Dalla Palma P, "Predictive value of ER1D5 antibody immunostaining in breast cancer". *Appl Immunohistochemistry* 1995; **3**: 85-90
- 9 Pertschuk LP, Feldman JG, Kim YD, Braithwaite L, Schneider F, Braverman AS, Axiotis C. Estrogen receptor immunocytochemistry in paraffin embedded tissues with ER1D5 predicts breast cancer endocrine response more accurately than H222Sp gamma in frozen sections or cytosol-based ligand-binding assays. *Cancer* 1996; **77**: 2514-2519
- 10 Brey EM, Lalani Z, Johnston C, Wong M, McIntire LV, Duke PJ, Patrick CW Jr. Automated selection of DAB-labeled tissue for immunohistochemical quantification. *J Histochem Cytochem* 2003; **51**: 575-584
- 11 Leal S, Diniz C, Sá C, Gonçalves J, Soares AS, Rocha-Pereira C, Fresco P. Semiautomated computer-assisted image analysis to quantify 3,3'-diaminobenzidine tetrahydrochloride-immunostained small tissues. *Anal Biochem* 2006; **357**: 137-143
- 12 Pham NA, Morrison A, Schwock J, Aviel-Ronen S, Iakovlev V, Tsao MS, Ho J, Hedley DW. Quantitative image analysis of immunohistochemical stains using a CMYK color model. *Diagn Pathol* 2007; **2**: 8
- 13 Matkowskyj KA, Cox R, Jensen RT, Benya RV. Quantitative immunohistochemistry by measuring cumulative signal strength accurately measures receptor number. *J Histochem Cytochem* 2003; **51**: 205-214
- 14 Aziz DC. Quantitation of estrogen and progesterone receptors by immunocytochemical and image analyses. *Am J Clin Pathol* 1992; **98**: 105-111
- 15 Auger M, Katz RL, Johnston DA, Sneige N, Ordonez NG, Fritsche H. Quantitation of immunocytochemical estrogen and progesterone receptor content in fine needle aspirates of breast carcinoma using the SAMBA 4000 image analysis system. *Anal Quant Cytol Histol* 1993; **15**: 274-280
- 16 Santeusano G, Mauriello A, Schiaroli S, Anemona L, Spagnoli LG, Scambia G, Oberholzer M. Densitometric and morphometric study of immunocytochemical estrogen receptors detection in breast carcinomas. *Pathol Res Pract* 1992; **188**: 478-483
- 17 Lehr HA, Mankoff DA, Corwin D, Santeusano G, Gown AM. Application of photoshop-based image analysis to quantification of hormone receptor expression in breast cancer. *J Histochem Cytochem* 1997; **45**: 1559-1565

- 18 **Ruifrok AC**, Katz RL, Johnston DA. Comparison of quantification of histochemical staining by hue-saturation-intensity (HSI) transformation and color-deconvolution. *Appl Immunohistochem Mol Morphol* 2003; **11**: 85-91
- 19 **Mofidi R**, Walsh R, Ridgway PF, Crotty T, McDermott EW, Keaveny TV, Duffy MJ, Hill AD, O'Higgins N. Objective measurement of breast cancer oestrogen receptor status through digital image analysis. *Eur J Surg Oncol* 2003; **29**: 20-24
- 20 **Hatanaka Y**, Hashizume K, Nitta K, Kato T, Itoh I, Tani Y. Cytometrical image analysis for immunohistochemical hormone receptor status in breast carcinomas. *Pathol Int* 2003; **53**: 693-699
- 21 **Kostopoulos S**, Cavouras D, Daskalakis A, Bougioukos P, Georgiadis P, Kagadis GC, Kalatzis I, Ravazoula P, Nikiforidis G. Colour-texture based image analysis method for assessing the hormone receptors status in breast tissue sections. *Conf Proc IEEE Eng Med Biol Soc* 2007; **2007**: 4985-4988
- 22 **Yeh IT**, Mies C. Application of immunohistochemistry to breast lesions. *Arch Pathol Lab Med* 2008; **132**: 349-358
- 23 **Remmele W**, Schicketanz KH. Immunohistochemical determination of estrogen and progesterone receptor content in human breast cancer. Computer-assisted image analysis (QIC score) vs. subjective grading (IRS). *Pathol Res Pract* 1993; **189**: 862-866
- 24 **Detre S**, Saclani Jotti G, Dowsett M. A "quickscore" method for immunohistochemical semiquantitation: validation for oestrogen receptor in breast carcinomas. *J Clin Pathol* 1995; **48**: 876-878
- 25 **Goedkoop AY**, de Rie MA, Teunissen MB, Picavet DI, van der Hall PO, Bos JD, Tak PP, Kraan MC. Digital image analysis for the evaluation of the inflammatory infiltrate in psoriasis. *Arch Dermatol Res* 2005; **297**: 51-59
- 26 **Kayser G**, Radziszowski D, Bzdyl P, Sommer R, Kayser K. Theory and implementation of an electronic, automated measurement system for images obtained from immunohistochemically stained slides. *Anal Quant Cytol Histol* 2006; **28**: 27-38
- 27 **Humm JL**, Macklis RM, Yang Y, Bump K, Chin LM. Image analysis for the study of radionuclide distribution in tissue sections. *J Nucl Med* 1994; **35**: 1217-1225
- 28 **Raisman-Vozari R**, Hirsch E, Javoy-Agid F, Vassort C, Savastata M, Feuerstein C, Thibault J, Agid Y. Quantitative autoradiography of tyrosine hydroxylase immunoreactivity in the rat brain. *J Neurochem* 1991; **57**: 1212-1222
- 29 **Lamaziere JM**, Lavallee J, Zunino C, Larrue J. Semiquantitative study of the distribution of two cellular antigens by computer-directed color analysis. *Lab Invest* 1993; **68**: 248-252
- 30 **Kim D**, Gregory CW, Smith GJ, Mohler JL. Immunohistochemical quantitation of androgen receptor expression using color video image analysis. *Cytometry* 1999; **35**: 2-10
- 31 **Diaz Encarnacion MM**, Griffin MD, Slezak JM, Bergstralh EJ, Stegall MD, Velosa JA, Grande JP. Correlation of quantitative digital image analysis with the glomerular filtration rate in chronic allograft nephropathy. *Am J Transplant* 2004; **4**: 248-256
- 32 **Charpin C**, Andrac L, Habib MC, Vacheret H, Xerri L, Devictor B, Lavaut MN, Toga M. Immunodetection in fine-needle aspirates and multiparametric (SAMBA) image analysis. Receptors (monoclonal antiestrogen and antiprogesterone) and growth fraction (monoclonal Ki67) evaluation in breast carcinomas. *Cancer* 1989; **63**: 863-872
- 33 **Pauschinger M**, Knopf D, Petschauer S, Doerner A, Poller W, Schwimmbeck PL, Kühl U, Schultheiss HP. Dilated cardiomyopathy is associated with significant changes in collagen type I/III ratio. *Circulation* 1999; **99**: 2750-2756
- 34 **Soukupova J**, Albrechtova J. Image analysis - tool for quantification of histochemical detections of phenolic compounds, lignin and peroxidases in needles of Norway spruce. *Biologica plantarum* 2003; **46**: 595-601
- 35 **Niendorf A**, Rath M, Wolf K, Peters S, Arps H, Beisiegel U, Dietel M. Morphological detection and quantification of lipoprotein(a) deposition in atheromatous lesions of human aorta and coronary arteries. *Virchows Arch A Pathol Anat Histopathol* 1990; **417**: 105-111
- 36 **Vrekoussis T**, Chaniotis V, Navrozoglou I, Dousias V, Pavlakis K, Stathopoulos EN, Zoras O. Image analysis of breast cancer immunohistochemistry-stained sections using ImageJ: an RGB-based model. *Anticancer Res* 2009; **29**: 4995-4998
- 37 **McCabe A**, Dolled-Filhart M, Camp RL, Rimm DL. Automated quantitative analysis (AQUA) of in situ protein expression, antibody concentration, and prognosis. *J Natl Cancer Inst* 2005; **97**: 1808-1815
- 38 **Chung GG**, Zerkowski MP, Ghosh S, Camp RL, Rimm DL. Quantitative analysis of estrogen receptor heterogeneity in breast cancer. *Lab Invest* 2007; **87**: 662-669
- 39 **Sharangpani GM**, Joshi AS, Porter K, Deshpande AS, Keyhani S, Naik GA, Gholap AS, Barsky SH. Semi-automated imaging system to quantitate estrogen and progesterone receptor immunoreactivity in human breast cancer. *J Microsc* 2007; **226**: 244-255

S- Editor Cheng JX L- Editor Webster JR E- Editor Ma WH

Acknowledgments to reviewers of *World Journal of Clinical Oncology*

Many reviewers have contributed their expertise and time to the peer review, a critical process to ensure the quality of *World Journal of Clinical Oncology*. The editors and authors of the articles submitted to the journal are grateful to the following reviewers for evaluating the articles (including those published in this issue and those rejected for this issue) during the last editing time period.

Songsak Petmitr, PhD, Associate Professor, Department of Tropical Nutrition and Food Science, Mahidol University, 420/6 Ratchawithi Road, Bangkok 10400, Thailand

Gary M Tse, MD, Department of Anatomical and Cellular Pathology, Prince of Wales Hospital, The Chinese University of Hong Kong, Shatin, Hong Kong, China

Ali Syed Arbab, MD, PhD, Associate Scientist and Director, Cellular and Molecular Imaging Laboratory, Department of Radiology, Henry Ford Hospital, 1 Ford Place, 2F, Box 82, Detroit, MI 48202, United States

Slimane Belbraouet, PhD, Professeur Titulaire, Directeur, École des sciences des aliments, de nutrition et d'études familiales, Université de Moncton, Moncton, NB, E1A 3E9, Canada

Yun Gong, MD, Associate Professor, Department of Pathology, Unit 53, The University of Texas, M D Anderson Cancer Center, 1515 Holcombe Blvd, Houston, TX77030, United States

Brendan Curran Stack, JR, MD, FACS, FACE, Chief, McGill Family Division of Clinical Research, Department of Otolaryngology-HNS, University of Arkansas for Medical Sciences, 4301 West Markham, Slot 543, Little Rock, AR 72205, United States

Meetings

Events Calendar 2011

January 13-14, 2011

3rd Breast-Gynecology International Cancer Conference BGICC, Cairo, Egypt

January 15-16, 2011

Melanoma 2011: 21st Annual Cutaneous Malignancy Update, San Diego, CA, United States

January 15, 2011

Current Trends in Breast Cancer: Updates From the 2010 San Antonio Breast Cancer Symposium, Dallas, TX, United States

January 20-22, 2011

Gastrointestinal Cancers Symposium 2011, San Francisco, CA, United States

January 21-23, 2011

8th Meeting of the EAU Section of Oncological Urology, London, England, United Kingdom

January 27-28, 2011

2nd National Conference: Recent Advances in Renal and Bladder Cancer, London, United Kingdom

January 27-28, 2011

8th Annual Cancer Drugs Research & Development, San Diego, CA, United States

February 10-12, 2011

17th Annual NOCR Meeting, Las Vegas, NV, United States

February 19-22, 2011

Scripps Cancer Center's 31st Annual Conference: Clinical Hematology and Oncology, San Diego, CA, United States

February 24-26, 2011

European Multidisciplinary Conference in Thoracic Oncology (Lung 2011-EMCTO), Lugano, Switzerland

February 25-27, 2011

7th European Congress on Hematologic Malignancies: From Clinical Science to Clinical Practice, Budapest, Hungary

March 02-05, 2011

64th Society of Surgical Oncology Annual Cancer Symposium 2011, San Antonio, TX, United States

March 04-06, 2011

8th Annual Oncology Nursing Advanced Practice: Innovation through Practice, San Diego, CA, United States

March 07-09, 2011

9th International Symposium on Targeted Anticancer Therapies, Paris, France

March 09-13, 2011

16th National Comprehensive Cancer Network Annual Conference (NCCN 2011), Hollywood, FL, United States

March 11-12, 2011

12th European Congress: Perspectives in Lung Cancer, Torino, Italy

March 14-18, 2011

Oncology Imaging Update in Costa Rica, Guanacaste, Costa Rica

March 17-19, 2011

International Cancer Prevention Update Symposium, New York, United States

March 18-22, 2011

Vienna, Austria
26th Annual EAU Congress

April 02-06, 2011

AACR 102nd Annual Meeting, Orlando, FL, United States

April 08-10, 2011

Asian Oncology Summit 2011, Hong Kong, China

April 20-23, 2011

9th International Gastric Cancer Congress, Seoul, South Korea

April 29-30, 2011

Cancer Survivorship Conference, Minneapolis, MN, United States

May 23-24, 2011

4th International Conference on Ovarian Cancer Screening, London, United Kingdom

June 03-07, 2011

47th American Society of Clinical Oncology Annual Meeting, Chicago, IL, United States

June 20-23, 2011

7th EADO Congress European Association of Dermato-Oncology, Nantes, France

June 22-25, 2011

ESMO Conference: 13th World Congress on Gastrointestinal Cancer, Barcelona, Spain

June 23-25, 2011

"MASCC/ISOO 2011 International

Symposium, Athens, Greece

July 03-07, 2011

14th World Conference on Lung Cancer, Amsterdam, Netherlands

July 14-17, 2011

3rd World Congress of the International Academy of Oral Oncology 2011, Singapore, Singapore

August 15-17, 2011

International Conference and Exhibition on Cancer Science & Therapy, Las Vegas, Nevada, United States

September 1-3, 2011

Tri-Society Head and Neck Oncology, Singapore, Singapore

September 7-10, 2011

Hallmarks and Horizons of Cancer, Lausanne, Switzerland

September 23-27, 2011

Joint 16th ECCO and 36th ESMO Multidisciplinary Cancer Congress, Stockholm, Sweden

October 06-07, 2011

Current Status and Future of Anti-Cancer Targeted Therapies, Buenos Aires, Argentina

November 30-December 03, 2011

AORTIC 2011-Entering the 21st Century for Cancer Control in Africa, Cairo, Egypt

November 6-9, 2011

NCRI Cancer Conference, Liverpool, United Kingdom

November 10-12, 2011

21st Asia Pacific Cancer Conference 2011, Kuala Lumpur, Wilayah Persekutuan, Malaysia

Instructions to authors

GENERAL INFORMATION

World Journal of Clinical Oncology (*World J Clin Oncol*, *WJCO*, online ISSN 2218-4333, DOI: 10.5306) is a monthly peer-reviewed, online, open-access (OA), journal supported by an editorial board consisting of 316 experts in oncology from 33 countries.

The biggest advantage of the OA model is that it provides free, full-text articles in PDF and other formats for experts and the public without registration, which eliminates the obstacle that traditional journals possess and usually delays the speed of the propagation and communication of scientific research results. The open access model has been proven to be a true approach that may achieve the ultimate goal of the journals, i.e. the maximization of the value to the readers, authors and society.

Maximization of personal benefits

The role of academic journals is to exhibit the scientific levels of a country, a university, a center, a department, and even a scientist, and build an important bridge for communication between scientists and the public. As we all know, the significance of the publication of scientific articles lies not only in disseminating and communicating innovative scientific achievements and academic views, as well as promoting the application of scientific achievements, but also in formally recognizing the "priority" and "copyright" of innovative achievements published, as well as evaluating research performance and academic levels. So, to realize these desired attributes of *WJCO* and create a well-recognized journal, the following four types of personal benefits should be maximized. The maximization of personal benefits refers to the pursuit of the maximum personal benefits in a well-considered optimal manner without violation of the laws, ethical rules and the benefits of others. (1) Maximization of the benefits of editorial board members: The primary task of editorial board members is to give a peer review of an unpublished scientific article *via* online office system to evaluate its innovativeness, scientific and practical values and determine whether it should be published or not. During peer review, editorial board members can also obtain cutting-edge information in that field at first hand. As leaders in their field, they have priority to be invited to write articles and publish commentary articles. We will put peer reviewers' names and affiliations along with the article they reviewed in the journal to acknowledge their contribution; (2) Maximization of the benefits of authors: Since *WJCO* is an open-access journal, readers around the world can immediately download and read, free of charge, high-quality, peer-reviewed articles from *WJCO* official website, thereby realizing the goals and significance of the communication between authors and peers as well as public reading; (3) Maximization of the benefits of readers: Readers can read or use, free of charge, high-quality peer-reviewed articles without any limits, and cite the arguments, viewpoints, concepts, theories, methods, results, conclusion or facts and data of pertinent literature so as to validate the innovativeness, scientific and practical values of their own research achievements, thus ensuring that their articles have novel arguments or viewpoints, solid evidence and correct conclusion; and (4) Maximization of the benefits of employees: It is an iron law that a first-class journal is unable to exist without first-class editors, and only first-class editors can create a first-class academic journal. We insist on strengthening our team cultivation and construction so that every employee, in an open, fair and transparent environment, could contribute their wisdom to edit and publish high-quality articles,

thereby realizing the maximization of the personal benefits of editorial board members, authors and readers, and yielding the greatest social and economic benefits.

Aims and scope

The aim of *WJCO* is to report rapidly new theories, methods and techniques for prevention, diagnosis, treatment, rehabilitation and nursing in the field of oncology. *WJCO* covers etiology, epidemiology, evidence-based medicine, informatics, diagnostic imaging, endoscopy, tumor recurrence and metastasis, tumor stem cells, radiotherapy, chemotherapy, interventional radiology, palliative therapy, clinical chemotherapy, biological therapy, minimally invasive therapy, physiotherapy, psycho-oncology, comprehensive therapy, oncology-related traditional medicine, integrated Chinese and Western medicine, and nursing. *WJCO* covers tumors in various organs/tissues, including the female reproductive system, bone and soft tissue, respiratory system, urinary system, endocrine system, skin, breast, nervous system, head and neck, digestive system, and hematologic and lymphatic system. The journal also publishes original articles and reviews that report the results of applied and basic research in fields related to oncology, such as immunology, physiopathology, cell biology, pharmacology, medical genetics, and pharmacology of Chinese herbs.

Columns

The columns in the issues of *WJCO* will include: (1) Editorial: To introduce and comment on major advances and developments in the field; (2) Frontier: To review representative achievements, comment on the state of current research, and propose directions for future research; (3) Topic Highlight: This column consists of three formats, including (A) 10 invited review articles on a hot topic, (B) a commentary on common issues of this hot topic, and (C) a commentary on the 10 individual articles; (4) Observation: To update the development of old and new questions, highlight unsolved problems, and provide strategies on how to solve the questions; (5) Guidelines for Basic Research: To provide Guidelines for basic research; (6) Guidelines for Clinical Practice: To provide guidelines for clinical diagnosis and treatment; (7) Review: To review systematically progress and unresolved problems in the field, comment on the state of current research, and make suggestions for future work; (8) Original Articles: To report innovative and original findings in oncology; (9) Brief Articles: To briefly report the novel and innovative findings in oncology; (10) Case Report: To report a rare or typical case; (11) Letters to the Editor: To discuss and make reply to the contributions published in *WJCO*, or to introduce and comment on a controversial issue of general interest; (12) Book Reviews: To introduce and comment on quality monographs of oncology; and (13) Guidelines: To introduce consensus and guidelines reached by international and national academic authorities worldwide on the research oncology.

Name of journal

World Journal of Clinical Oncology

ISSN

ISSN 2218-4333 (online)

Indexed and Abstracted in

PubMed Central, PubMed, Digital Object Identifier, and Directory of Open Access Journals.

Published by

Baishideng Publishing Group Co., Limited

SPECIAL STATEMENT

All articles published in this journal represent the viewpoints of the authors except where indicated otherwise.

Biostatistical editing

Statistical review is performed after peer review. We invite an expert in Biomedical Statistics from to evaluate the statistical method used in the paper, including *t*-test (group or paired comparisons), chi-squared test, Ridit, probit, logit, regression (linear, curvilinear, or stepwise), correlation, analysis of variance, analysis of covariance, *etc.* The reviewing points include: (1) Statistical methods should be described when they are used to verify the results; (2) Whether the statistical techniques are suitable or correct; (3) Only homogeneous data can be averaged. Standard deviations are preferred to standard errors. Give the number of observations and subjects (*n*). Losses in observations, such as drop-outs from the study should be reported; (4) Values such as ED50, LD50, IC50 should have their 95% confidence limits calculated and compared by weighted probit analysis (Bliss and Finney); and (5) The word 'significantly' should be replaced by its synonyms (if it indicates extent) or the *P* value (if it indicates statistical significance).

Conflict-of-interest statement

In the interests of transparency and to help reviewers assess any potential bias, *WJCO* requires authors of all papers to declare any competing commercial, personal, political, intellectual, or religious interests in relation to the submitted work. Referees are also asked to indicate any potential conflict they might have reviewing a particular paper. Before submitting, authors are suggested to read "Uniform Requirements for Manuscripts Submitted to Biomedical Journals: Ethical Considerations in the Conduct and Reporting of Research: Conflicts of Interest" from International Committee of Medical Journal Editors (ICMJE), which is available at: http://www.icmje.org/ethical_4conflicts.html.

Sample wording: [Name of individual] has received fees for serving as a speaker, a consultant and an advisory board member for [names of organizations], and has received research funding from [names of organization]. [Name of individual] is an employee of [name of organization]. [Name of individual] owns stocks and shares in [name of organization]. [Name of individual] owns patent [patent identification and brief description].

Statement of informed consent

Manuscripts should contain a statement to the effect that all human studies have been reviewed by the appropriate ethics committee or it should be stated clearly in the text that all persons gave their informed consent prior to their inclusion in the study. Details that might disclose the identity of the subjects under study should be omitted. Authors should also draw attention to the Code of Ethics of the World Medical Association (Declaration of Helsinki, 1964, as revised in 2004).

Statement of human and animal rights

When reporting the results from experiments, authors should follow the highest standards and the trial should conform to Good Clinical Practice (for example, US Food and Drug Administration Good Clinical Practice in FDA-Regulated Clinical Trials; UK Medicines Research Council Guidelines for Good Clinical Practice in Clinical Trials) and/or the World Medical Association Declaration of Helsinki. Generally, we suggest authors follow the lead investigator's national standard. If doubt exists whether the research was conducted in accordance with the above standards, the authors must explain the rationale for their approach and demonstrate that the institutional review body explicitly approved the doubtful aspects of the study.

Before submitting, authors should make their study approved by the relevant research ethics committee or institutional review board. If human participants were involved, manuscripts must be accompanied by a statement that the experiments were undertaken with the understanding and appropriate informed consent of each. Any personal item or information will not be published without explicit consents from the involved patients. If experimental animals were used, the materials and methods (experimental procedures) section must

clearly indicate that appropriate measures were taken to minimize pain or discomfort, and details of animal care should be provided.

SUBMISSION OF MANUSCRIPTS

Manuscripts should be typed in 1.5 line spacing and 12 pt. Book Antiqua with ample margins. Number all pages consecutively, and start each of the following sections on a new page: Title Page, Abstract, Introduction, Materials and Methods, Results, Discussion, Acknowledgements, References, Tables, Figures, and Figure Legends. Neither the editors nor the publisher are responsible for the opinions expressed by contributors. Manuscripts formally accepted for publication become the permanent property of Baishideng Publishing Group Co., Limited, and may not be reproduced by any means, in whole or in part, without the written permission of both the authors and the publisher. We reserve the right to copy-edit and put onto our website accepted manuscripts. Authors should follow the relevant guidelines for the care and use of laboratory animals of their institution or national animal welfare committee. For the sake of transparency in regard to the performance and reporting of clinical trials, we endorse the policy of the ICMJE to refuse to publish papers on clinical trial results if the trial was not recorded in a publicly-accessible registry at its outset. The only register now available, to our knowledge, is <http://www.clinicaltrials.gov> sponsored by the United States National Library of Medicine and we encourage all potential contributors to register with it. However, in the case that other registers become available you will be duly notified. A letter of recommendation from each author's organization should be provided with the contributed article to ensure the privacy and secrecy of research is protected.

Authors should retain one copy of the text, tables, photographs and illustrations because rejected manuscripts will not be returned to the author(s) and the editors will not be responsible for loss or damage to photographs and illustrations sustained during mailing.

Online submissions

Manuscripts should be submitted through the Online Submission System at: <http://www.wjgnet.com/2218-4333office>. Authors are highly recommended to consult the ONLINE INSTRUCTIONS TO AUTHORS (http://www.wjgnet.com/2218-4333/g_info_20100722172206.htm) before attempting to submit online. For assistance, authors encountering problems with the Online Submission System may send an email describing the problem to wjco@wjgnet.com, or by telephone: +86-10-85381892. If you submit your manuscript online, do not make a postal contribution. Repeated online submission for the same manuscript is strictly prohibited.

MANUSCRIPT PREPARATION

All contributions should be written in English. All articles must be submitted using word-processing software. All submissions must be typed in 1.5 line spacing and 12 pt. Book Antiqua with ample margins. Style should conform to our house format. Required information for each of the manuscript sections is as follows:

Title page

Title: Title should be less than 12 words.

Running title: A short running title of less than 6 words should be provided.

Authorship: Authorship credit should be in accordance with the standard proposed by International Committee of Medical Journal Editors, based on (1) substantial contributions to conception and design, acquisition of data, or analysis and interpretation of data; (2) drafting the article or revising it critically for important intellectual content; and (3) final approval of the version to be published. Authors should meet conditions 1, 2, and 3.

Institution: Author names should be given first, then the complete name of institution, city, province and postcode. For example, Xu-Chen Zhang, Li-Xin Mei, Department of Pathology, Chengde Medical College, Chengde 067000, Hebei Province, China. One author may be represented from two institutions, for example, George

Sgourakis, Department of General, Visceral, and Transplantation Surgery, Essen 45122, Germany; George Sgourakis, 2nd Surgical Department, Korgialenio-Benakio Red Cross Hospital, Athens 15451, Greece

Author contributions: The format of this section should be: Author contributions: Wang CL and Liang L contributed equally to this work; Wang CL, Liang L, Fu JF, Zou CC, Hong F and Wu XM designed the research; Wang CL, Zou CC, Hong F and Wu XM performed the research; Xue JZ and Lu JR contributed new reagents/analytic tools; Wang CL, Liang L and Fu JF analyzed the data; and Wang CL, Liang L and Fu JF wrote the paper.

Supportive foundations: The complete name and number of supportive foundations should be provided, e.g. Supported by National Natural Science Foundation of China, No. 30224801

Correspondence to: Only one corresponding address should be provided. Author names should be given first, then author title, affiliation, the complete name of institution, city, postcode, province, country, and email. All the letters in the email should be in lower case. A space interval should be inserted between country name and email address. For example, Montgomery Bissell, MD, Professor of Medicine, Chief, Liver Center, Gastroenterology Division, University of California, Box 0538, San Francisco, CA 94143, United States. montgomery.bissell@ucsf.edu

Telephone and fax: Telephone and fax should consist of +, country number, district number and telephone or fax number, e.g. Telephone: +86-10-59080039 Fax: +86-10-85381893

Peer reviewers: All articles received are subject to peer review. Normally, three experts are invited for each article. Decision for acceptance is made only when at least two experts recommend an article for publication. Reviewers for accepted manuscripts are acknowledged in each manuscript, and reviewers of articles which were not accepted will be acknowledged at the end of each issue. To ensure the quality of the articles published in *WJCO*, reviewers of accepted manuscripts will be announced by publishing the name, title/position and institution of the reviewer in the footnote accompanying the printed article. For example, reviewers: Professor Jing-Yuan Fang, Shanghai Institute of Digestive Disease, Shanghai, Affiliated Renji Hospital, Medical Faculty, Shanghai Jiaotong University, Shanghai, China; Professor Xin-Wei Han, Department of Radiology, The First Affiliated Hospital, Zhengzhou University, Zhengzhou, Henan Province, China; and Professor Anren Kuang, Department of Nuclear Medicine, Huaxi Hospital, Sichuan University, Chengdu, Sichuan Province, China.

Abstract

There are unstructured abstracts (no more than 256 words) and structured abstracts (no more than 480). The specific requirements for structured abstracts are as follows:

An informative, structured abstracts of no more than 480 words should accompany each manuscript. Abstracts for original contributions should be structured into the following sections. AIM (no more than 20 words): Only the purpose should be included. Please write the aim as the form of "To investigate/study/..."; MATERIALS AND METHODS (no more than 140 words); RESULTS (no more than 294 words): You should present *P* values where appropriate and must provide relevant data to illustrate how they were obtained, e.g. 6.92 ± 3.86 vs 3.61 ± 1.67 , $P < 0.001$; CONCLUSION (no more than 26 words).

Key words

Please list 5-10 key words, selected mainly from *Index Medicus*, which reflect the content of the study.

Text

For articles of these sections, original articles and brief articles, the main text should be structured into the following sections: INTRO-

DUCTION, MATERIALS AND METHODS, RESULTS and DISCUSSION, and should include appropriate Figures and Tables. Data should be presented in the main text or in Figures and Tables, but not in both. The main text format of these sections, editorial, topic highlight, case report, letters to the editors, can be found at: http://www.wjgnet.com/2218-4333/g_info_list.htm.

Illustrations

Figures should be numbered as 1, 2, 3, *etc.*, and mentioned clearly in the main text. Provide a brief title for each figure on a separate page. Detailed legends should not be provided under the figures. This part should be added into the text where the figures are applicable. Figures should be either Photoshop or Illustrator files (in tiff, eps, jpeg formats) at high-resolution. Examples can be found at: <http://www.wjgnet.com/1007-9327/13/4520.pdf>; <http://www.wjgnet.com/1007-9327/13/4554.pdf>; <http://www.wjgnet.com/1007-9327/13/4891.pdf>; <http://www.wjgnet.com/1007-9327/13/4986.pdf>; <http://www.wjgnet.com/1007-9327/13/4498.pdf>. Keeping all elements compiled is necessary in line-art image. Scale bars should be used rather than magnification factors, with the length of the bar defined in the legend rather than on the bar itself. File names should identify the figure and panel. Avoid layering type directly over shaded or textured areas. Please use uniform legends for the same subjects. For example: Figure 1 Pathological changes in atrophic gastritis after treatment. A: ...; B: ...; C: ...; D: ...; E: ...; F: ...; G: ... *etc.* It is our principle to publish high resolution-figures for the printed and E-versions.

Tables

Three-line tables should be numbered 1, 2, 3, *etc.*, and mentioned clearly in the main text. Provide a brief title for each table. Detailed legends should not be included under tables, but rather added into the text where applicable. The information should complement, but not duplicate the text. Use one horizontal line under the title, a second under column heads, and a third below the Table, above any footnotes. Vertical and italic lines should be omitted.

Notes in tables and illustrations

Data that are not statistically significant should not be noted. ^a*P* < 0.05, ^b*P* < 0.01 should be noted (*P* > 0.05 should not be noted). If there are other series of *P* values, ^c*P* < 0.05 and ^d*P* < 0.01 are used. A third series of *P* values can be expressed as ^e*P* < 0.05 and ^f*P* < 0.01. Other notes in tables or under illustrations should be expressed as ¹F, ²F, ³F; or sometimes as other symbols with a superscript (Arabic numerals) in the upper left corner. In a multi-curve illustration, each curve should be labeled with ●, ○, ■, □, ▲, △, *etc.*, in a certain sequence.

Acknowledgments

Brief acknowledgments of persons who have made genuine contributions to the manuscript and who endorse the data and conclusions should be included. Authors are responsible for obtaining written permission to use any copyrighted text and/or illustrations.

REFERENCES

Coding system

The author should number the references in Arabic numerals according to the citation order in the text. Put reference numbers in square brackets in superscript at the end of citation content or after the cited author's name. For citation content which is part of the narration, the coding number and square brackets should be typeset normally. For example, "Crohn's disease (CD) is associated with increased intestinal permeability^[1,2]". If references are cited directly in the text, they should be put together within the text, for example, "From references^[19,22-24], we know that..."

When the authors write the references, please ensure that the order in text is the same as in the references section, and also ensure the spelling accuracy of the first author's name. Do not list the same citation twice.

Instructions to authors

PMID and DOI

Pleased provide PubMed citation numbers to the reference list, e.g. PMID and DOI, which can be found at <http://www.ncbi.nlm.nih.gov/sites/entrez?db=pubmed> and <http://www.crossref.org/SimpleTextQuery/>, respectively. The numbers will be used in E-version of this journal.

Style for journal references

Authors: the name of the first author should be typed in bold-faced letters. The family name of all authors should be typed with the initial letter capitalized, followed by their abbreviated first and middle initials. (For example, Lian-Sheng Ma is abbreviated as Ma LS, Bo-Rong Pan as Pan BR). The title of the cited article and italicized journal title (journal title should be in its abbreviated form as shown in PubMed), publication date, volume number (in black), start page, and end page [PMID: 11819634 DOI: 10.3748/wjg.13.5396].

Style for book references

Authors: the name of the first author should be typed in bold-faced letters. The surname of all authors should be typed with the initial letter capitalized, followed by their abbreviated middle and first initials. (For example, Lian-Sheng Ma is abbreviated as Ma LS, Bo-Rong Pan as Pan BR) Book title. Publication number. Publication place: Publication press, Year: start page and end page.

Format

Journals

English journal article (list all authors and include the PMID where applicable)

- 1 **Jung EM**, Clevert DA, Schreyer AG, Schmitt S, Rennert J, Kubale R, Feuerbach S, Jung F. Evaluation of quantitative contrast harmonic imaging to assess malignancy of liver tumors: A prospective controlled two-center study. *World J Gastroenterol* 2007; **13**: 6356-6364 [PMID: 18081224 DOI: 10.3748/wjg.13.6356]

Chinese journal article (list all authors and include the PMID where applicable)

- 2 **Lin GZ**, Wang XZ, Wang P, Lin J, Yang FD. Immunologic effect of Jianpi Yishen decoction in treatment of Pixu-diarhoea. *Shijie Huaren Xiaohua Zazhi* 1999; **7**: 285-287

In press

- 3 **Tian D**, Araki H, Stahl E, Bergelson J, Kreitman M. Signature of balancing selection in Arabidopsis. *Proc Natl Acad Sci USA* 2006; In press

Organization as author

- 4 **Diabetes Prevention Program Research Group**. Hypertension, insulin, and proinsulin in participants with impaired glucose tolerance. *Hypertension* 2002; **40**: 679-686 [PMID: 12411462 PMID:2516377 DOI:10.1161/01.HYP.0000035706.28494.09]

Both personal authors and an organization as author

- 5 **Vallancien G**, Emberton M, Harving N, van Moorselaar RJ; Alf-One Study Group. Sexual dysfunction in 1, 274 European men suffering from lower urinary tract symptoms. *J Urol* 2003; **169**: 2257-2261 [PMID: 12771764 DOI:10.1097/01.ju.0000067940.76090.73]

No author given

- 6 21st century heart solution may have a sting in the tail. *BMJ* 2002; **325**: 184 [PMID: 12142303 DOI:10.1136/bmj.325.7357.184]

Volume with supplement

- 7 **Geraud G**, Spierings EL, Keywood C. Tolerability and safety of frovatriptan with short- and long-term use for treatment of migraine and in comparison with sumatriptan. *Headache* 2002; **42** Suppl 2: S93-99 [PMID: 12028325 DOI:10.1046/j.1526-4610.42.s2.7.x]

Issue with no volume

- 8 **Banit DM**, Kaufer H, Hartford JM. Intraoperative frozen section analysis in revision total joint arthroplasty. *Clin Orthop Relat Res* 2002; (**401**): 230-238 [PMID: 12151900 DOI:10.1097/00003086-200208000-00026]

No volume or issue

- 9 Outreach: Bringing HIV-positive individuals into care. *HRS-A Careaction* 2002; 1-6 [PMID: 12154804]

Books

Personal author(s)

- 10 **Sherlock S**, Dooley J. Diseases of the liver and biliary system. 9th ed. Oxford: Blackwell Sci Pub, 1993: 258-296

Chapter in a book (list all authors)

- 11 **Lam SK**. Academic investigator's perspectives of medical treatment for peptic ulcer. In: Swabb EA, Azabo S. Ulcer disease: investigation and basis for therapy. New York: Marcel Dekker, 1991: 431-450

Author(s) and editor(s)

- 12 **Breedlove GK**, Schorfheide AM. Adolescent pregnancy. 2nd ed. Wiczorek RR, editor. White Plains (NY): March of Dimes Education Services, 2001: 20-34

Conference proceedings

- 13 **Harnden P**, Joffe JK, Jones WG, editors. Germ cell tumours V. Proceedings of the 5th Germ cell tumours Conference; 2001 Sep 13-15; Leeds, UK. New York: Springer, 2002: 30-56

Conference paper

- 14 **Christensen S**, Oppacher F. An analysis of Koza's computational effort statistic for genetic programming. In: Foster JA, Lutton E, Miller J, Ryan C, Tettamanzi AG, editors. Genetic programming. EuroGP 2002: Proceedings of the 5th European Conference on Genetic Programming; 2002 Apr 3-5; Kinsdale, Ireland. Berlin: Springer, 2002: 182-191

Electronic journal (list all authors)

- 15 Morse SS. Factors in the emergence of infectious diseases. *Emerg Infect Dis* serial online, 1995-01-03, cited 1996-06-05; 1(1): 24 screens. Available from: URL: <http://www.cdc.gov/ncidod/eid/index.htm>

Patent (list all authors)

- 16 **Pagedas AC**, inventor; Ancel Surgical R&D Inc., assignee. Flexible endoscopic grasping and cutting device and positioning tool assembly. United States patent US 20020103498. 2002 Aug 1

Statistical data

Write as mean \pm SD or mean \pm SE.

Statistical expression

Express *t* test as *t* (in italics), *F* test as *F* (in italics), chi square test as χ^2 (in Greek), related coefficient as *r* (in italics), degree of freedom as *v* (in Greek), sample number as *n* (in italics), and probability as *P* (in italics).

Units

Use SI units. For example: body mass, *m* (B) = 78 kg; blood pressure, *p* (B) = 16.2/12.3 kPa; incubation time, *t* (incubation) = 96 h, blood glucose concentration, *c* (glucose) 6.4 \pm 2.1 mmol/L; blood CEA mass concentration, *p* (CEA) = 8.6 24.5 μ g/L; CO₂ volume fraction, 50 mL/L CO₂, not 5% CO₂; likewise for 40 g/L formaldehyde, not 10% formalin; and mass fraction, 8 ng/g, etc. Arabic numerals such as 23, 243, 641 should be read 23 243 641.

The format for how to accurately write common units and quantum numbers can be found at: http://www.wjgnet.com/2218-4333/g_info_20110723153305.htm.

Abbreviations

Standard abbreviations should be defined in the abstract and on first mention in the text. In general, terms should not be abbreviated unless they are used repeatedly and the abbreviation is helpful to the reader. Permissible abbreviations are listed in Units, Symbols and Abbreviations: A Guide for Biological and Medical Editors and Authors (Ed. Baron DN, 1988) published by The Royal Society of Medicine, London. Certain commonly used abbreviations, such as DNA, RNA, HIV, LD50, PCR, HBV, ECG, WBC, RBC, CT, ESR, CSF, IgG, ELISA, PBS, ATP, EDTA, mAb, can be used directly without further explanation.

Italics

Quantities: *t* time or temperature, *c* concentration, *A* area, *l* length, *m* mass, *V* volume.
 Genotypes: *gyrA*, *arg 1*, *c myc*, *c fos*, etc.
 Restriction enzymes: *EcoRI*, *HindII*, *BamHI*, *Kbo I*, *Kpn I*, etc.
 Biology: *H. pylori*, *E. coli*, etc.

Examples for paper writing

Editorial: http://www.wjgnet.com/2218-4333/g_info_20100723140942.htm

Frontier: http://www.wjgnet.com/2218-4333/g_info_20100723141035.htm

Topic highlight: http://www.wjgnet.com/2218-4333/g_info_20100723141239.htm

Observation: http://www.wjgnet.com/2218-4333/g_info_20100723141532.htm

Guidelines for basic research: http://www.wjgnet.com/2218-4333/g_info_20100723142040.htm

Guidelines for clinical practice: http://www.wjgnet.com/2218-5836/g_info_20100723142248.htm

Review: http://www.wjgnet.com/2218-4333/g_info_20100723145519.htm

Original articles: http://www.wjgnet.com/2218-4333/g_info_20100723145856.htm

Brief articles: http://www.wjgnet.com/2218-4333/g_info_20100723150253.htm

Case report: http://www.wjgnet.com/2218-4333/g_info_20100723150420.htm

Letters to the editor: http://www.wjgnet.com/2218-4333/g_info_20100723150642.htm

Book reviews: http://www.wjgnet.com/2218-4333/g_info_20100723150839.htm

Guidelines: http://www.wjgnet.com/2218-4333/g_info_20100723150924.htm

SUBMISSION OF THE REVISED MANUSCRIPTS AFTER ACCEPTED

Please revise your article according to the revision policies of *WJCO*. The revised version including manuscript and high-resolution image figures (if any) should be copied on a floppy or compact disk. The author should send the revised manuscript, along with printed high-resolution color or black and white photos, copyright transfer letter, and responses to the reviewers by courier (such as EMS/DHL).

Editorial Office

World Journal of Clinical Oncology
 Editorial Department: Room 903, Building D,

Ocean International Center,
 No. 62 Dongsihuan Zhonglu,
 Chaoyang District, Beijing 100025, China
 E-mail: wjco@wjgnet.com
<http://www.wjgnet.com>
 Telephone: +86-10-8538-1892
 Fax: +86-10-8538-1893

Language evaluation

The language of a manuscript will be graded before it is sent for revision. (1) Grade A: priority publishing; (2) Grade B: minor language polishing; (3) Grade C: a great deal of language polishing needed; and (4) Grade D: rejected. Revised articles should reach Grade A or B.

Copyright assignment form

Please download a Copyright assignment form from http://www.wjgnet.com/2218-4333/g_info_20100723153117.htm.

Responses to reviewers

Please revise your article according to the comments/suggestions provided by the reviewers. The format for responses to the reviewers' comments can be found at: http://www.wjgnet.com/2218-4333/g_info_20100723152755.htm.

Proof of financial support

For paper supported by a foundation, authors should provide a copy of the document and serial number of the foundation.

Links to documents related to the manuscript

WJCO will be initiating a platform to promote dynamic interactions between the editors, peer reviewers, readers and authors. After a manuscript is published online, links to the PDF version of the submitted manuscript, the peer-reviewers' report and the revised manuscript will be put on-line. Readers can make comments on the peer reviewer's report, authors' responses to peer reviewers, and the revised manuscript. We hope that authors will benefit from this feedback and be able to revise the manuscript accordingly in a timely manner.

Science news releases

Authors of accepted manuscripts are suggested to write a science news item to promote their articles. The news will be released rapidly at EurekAlert/AAAS (<http://www.eurekalert.org>). The title for news items should be less than 90 characters; the summary should be less than 75 words; and main body less than 500 words. Science news items should be lawful, ethical, and strictly based on your original content with an attractive title and interesting pictures.

Publication fee

WJCO is an international, peer-reviewed, Open-Access, online journal. Articles published by this journal are distributed under the terms of the Creative Commons Attribution Non-commercial License, which permits use, distribution, and reproduction in any medium, provided the original work is properly cited, the use is non commercial and is otherwise in compliance with the license. Authors of accepted articles must pay a publication fee. The related standards are as follows. Publication fee: 1300 USD per article. Editorial, topic highlights, book reviews and letters to the editor are published free of charge.